

18 July 95

SUBJECT: Field Trip to Barren Island, Chesapeake Bay, Maryland for Geotube Application

1. On Wednesday, 24 May 95, I visited Barren Island to witness the installation of geotubes along a portion of an eroded shoreline. Dr. Mary Landin (EL) and Jack Davis (CERC) also made the trip. We met with Bob Blama (Baltimore District, Navigation Branch). Mr. Blama briefed us on the purposes of this geotube placement and provided us with transportation to the island so that we could witness the placement of the pumped dredge material within the tubes. Three tubes, one black in color and two white ones had been previously placed a day or two before our visit. The black colored tube was constructed of a fabric of less tensile strength than the white ones. The accompanying photos illustrate the process of bag placement. Photo 1 shows the previously placed tubes; the black one being laid perpendicular to and outward from the shore of the island, and the two white ones being placed parallel to the shoreline. The abutment between the two white tubes is approximately at the location of the crossing dredge pipe. Each of the tubes were 200 ft in length (and either 30 or 37 ft in circumference). Photo 2 gives a view in the vicinity of the juncture between two tubes. The dredge pipe is being dragged to the location of the to-be-placed tube. Photo 3 is the view from a position on the black tube. The new tube will be placed just beyond the group of standing men and alongside the barge mounted crane. The tubes are being placed to provide a containment area for dredged material, and will also provide wave erosion protection for the island's shoreline.

2. Photo 4 shows the method of tube deployment. The tube fabric was delivered on a roll; the crane hoisted a length (probably 25 ft) and the bag was towed toward its final position. This hoisting and towing process was continued until the full 200 foot length was deployed. Then, one end of the tube was pulled, as shown in Photo 5, until it abutted the end of the previously placed tube. After the tube was positioned, the dredge pipe elbow was inserted into one of the fabric sleeves sewn into various locations along the tube as shown in Photo 6, and pumping commenced.

3. After about five hours of pumping a sandy material (from the shipping channel) the tube had emerged and rose above the surface as shown in Photo 7. The dredge unit, shown in Photo 8, was located about a mile from the island. Operators on the dredge estimated that the pumping pressure (at the dredge) was about 8-10 psi. Although fabric sleeves for filling were manufactured about every fifty feet along the tube, the entire tube length of 200 ft was filled from one filling position. Also notice in Photo 7 that slurry is exiting from a "vent" sleeve in the end of the tube. Photos 9 and 10 show the tubes at the end of the filling process. Photo 10 also shows two men walking on the "bottom" alongside the tube. Based on this photo, it is estimated that the total height of the filled tube is approximately 5 to 5.5 ft (since the men's heads are slightly above the tube and the photo was taken from the shore at a height of about 6 ft above the sea elevation).

4. This past January a Distinct Element (DE) code which I had written many years ago for

scour studies was modified and adapted to simulate the experience at Marina Del Rey, California, where sand-filled geotubes had become stuck during discharge from a bottom-dump scow. These simulations accurately predicted the "payload" of dredged material which could successfully be discharged from that particular scow. After the trip to Barren Island, I became curious about whether the DE code could also be profitably applied to simulating the filling of geotubes. At present, there exists very little capability to examine the forces and displacements of and within geotubes throughout a particular application process. Indeed, one of the few techniques known to me is a capability to compute the tensile forces within the walls of a long, constant cross-section flexible-walled tank (or membrane) filled with a fluid. A simple computer program entitled TANK was written which, given any two of the tensile force, T , the excess water pressure (as though a sealed stand pipe were inserted into the top of the tank) above the top of the tank, P_0 , or the circumference of the tank, C , will compute the one not specified. The solution¹ for this problem is predicated on the fact that the radius of curvature, r , of any unsupported point on the periphery of the membrane-like tank is, from static equilibrium considerations, given exactly as $r=T/P$, where P is the total pressure (i.e. $P=P_0+\gamma H$, where H is the distance below the top of the tank, and γ is the density of the fluid) at any elevation within the tank. Figure 1 shows the solution for three cases; a) where the circumference of the tank was specified as 37 ft and the excess water pressure above the top of the tank as 8 ft (of water) or 3.467 psi; b) for the same circumference but an excess pressure of 15 ft (or 6.5 psi); and c) for an excess pressure of 3 ft or 1.30 psi. The computer program yielded the other parameters printed on both pages of the figure; e.g., for an 8 ft head, the tension force in the tube (which is constant everywhere in the membrane) is 316.4 lbs/in., the height of the tube is 9.53 ft, etc. Increasing the excess head, P_0 , to 15 ft, increases the tension force to 537.1 lbs/in. and the height of the tube to 10.26 ft. Decreasing the excess head to 3 ft reduces the tension force to 151 lbs/in. and reduces the tube height to 8.19 ft. The problem with the predictions of a code which relies on this (entirely correct) membrane theory is that it will always greatly overestimate the actual tension force and height of tube since it is presumed that the tube does not leak and can maintain any applied internal pressure. Although there are applications, such as the use of fluid filled impermeable tubes utilized for temporary dikes and walls (a subject which will be further discussed in paragraph 11), for which this simple membrane theory is appropriate, most geotube applications employ fabrics that provide for free or considerable drainage of water. For this reason, it is unreasonable to expect that the tension forces and tube heights would nearly approach those predicted for hydrostatic conditions.

5. In order to more realistically simulate the pumping of dredged material (sand) into permeable geotubes, the DE code used for the Marina Del Rey application was further modified so that the injection of disc-shaped elements (which represent the sand) into a membrane consisting of connected (and therefore able to support tension forces) discs. Each

¹See Den Hartog, J. P., *Advanced Strength of Materials*, McGraw-Hill Book Company, Inc., 1952. A graphical construction procedure to solve this equation is presented. This graphical technique is easily computerized if the given parameters are T and P . If parameters T and C , or P and C , are given, an iterative procedure (in which trial estimates of P or T , respectively, are chosen) also provides an accurate solution.

membrane element is connected to two other membrane neighbors. The membrane elements are capable of transferring compressive and tensile forces (to their membrane neighbors), but they do not transfer any friction caused shear forces to their membrane neighbors. They are generally free to move in all directions, but they are restricted from rotation. This rotation restriction results in shearing forces (which are derived from frictional properties) to be transferred to all other non-membrane contacted elements. The shearing force at contacts are limited by Amonton's Law, $S \leq N \tan \phi$, where S is the shear force, N is normal (compressive) force at the contact and ϕ is the appropriate angle of internal friction. In physics nomenclature, the coefficient of friction, μ , is equivalent to $\tan \phi$. Photo 11 shows a very early stage of one of the simulations. The rectangular shaped collection of discs (black in color) forms the membrane. The circumference (or, more correctly, the perimeter length) of the membrane (for this and all other simulations) was set at 37 ft. The red colored discs represent the sand which has so far been injected. These "sand" elements are free to move in all directions and are also free to rotate. They can transfer shear forces and compressive (only) normal forces. The elongated bar shaped elements (those near the centerline of the tube with the "+" symbols at their centers) were used to "pump," in a piston-like fashion, the particles into the tube. The red discs located near the top of the photo provide a reservoir of particles which are moved one row at a time to a position below the "pump" elements. A downward directed load was imposed on the "pump" elements and this load caused those two elements to move downward and to force any disc elements making contact with the "pump" elements to be injected into the tube. As soon it was detected that the "pump" elements achieved a position below the tube neck (the 4th discs down from the top opening of the membrane), the "pump" elements were repositioned upward (and adjacent to the 3rd tube neck elements down), a row of reservoir elements were inserted under the "pump", and the process repeated over and over until the tube would accept no more injected particles (i.e., until the downward pressure on the "pump" was insufficient to force more particles into the tube). The top border of the photo contains information pertinent to the "run". Notice that the time, t , is given as 0.3266 sec, the time step increment, dt , is 0.000041 sec, and the number of iteration cycles thus far is 7980. The combination of numbers $0/1.00/1.00/30/30 \% = 2.78$ is significant in that the 30/30 sequence refers to coefficients of internal friction, ϕ , applicable to the sand. The first 30° refers to the friction coefficient applied between sand particles, and the second refers to the friction angle between the membrane and the elements on which the membrane rests (although it is not apparent in the photo, the base of the tube is resting on a very long horizontal "bar" element). The $\% = 2.78$ indicates that the picture we are seeing corresponds to time which is 2.78% of the total time of the simulation. The photo also has visible a "decimal three-hand clock" located on the right edge. The shortest hand shows the whole seconds, the middle hands shows tenths of seconds, and the long hand indicates hundredths of seconds (i.e. read as 0.32 sec).

6. Photos 12-16 show the sequence of tube shapes which occurred as the tube was filled. For this series of photos, the applied "pump" head was set equal to 8 ft of water head (or 3.47 psi). Photo 12 shows the situation after 2.58 sec of injection. Up to this point, all of the movement of the tube is caused by the physical movement and membrane expansion forces of the injected discs. The distance between each of the grid lines (in both the vertical and horizontal directions) is 0.8 ft. The green shaded zone covering the bottom 2 ft (about

2.5 grids in height) represents the water level used during the simulation. Within this zone, buoyant unit weights were assigned to the disc elements (the membrane elements were considered to be weightless and not subject to buoyancy forces). The density of the "sand" discs was set to 2.6 gm/cc; the diameter of the "sand" grains was set at 5.54 cm, and the mass of each grain was 62.69 gm. It is the hypothesis of this writer that membrane inflation is primarily the result of movements caused by grain to grain contacts and not simply hydrostatic pressures (since the tube is constantly draining and/or vented). However, provision was made to include a purely fluid-caused pressure on those portions of the tube lying below the elevation of particles contained at any given time within the tube. That is, an outward pressure was imposed normal to the inner surface of the tube which is caused by the head caused by the difference in elevation of the tube neck (4th element down) and the elevation of any element forming the membrane. For any membrane elements, located below the water surface there was no applied internal fluid pressure since the water pressure outside the membrane will cancel the effects. The application of internal pressure in this manner will not cause the tube to self-inflate as a result of fluid forces since the applied pressures for membrane elements will be zero for any elements located at or above the current elevation of the tube neck. However, as particle to particle interactions cause the tube neck to rise (above the elevation of the water) the internally applied fluid pressure will go into effect. The tube filling process is followed in Photos 13-15 and finally, as shown in Photo 16, after a time of 7.6499 sec, the "pump" head of 8 ft of water is not sufficient to inject any more particles against the tensile forces which are created in the membrane.

7. As the simulation is carried out, output data are stored which may be used to prepare various plots. Figure 2a is a plot of the mass of injected particles (for a one cm thick cross-section of tube) versus time. (In fact, the mass of injected particles should be doubled since the simulation took advantage of symmetry about the tube's centerline, and the code was not modified to double this number when printed.) This mass of injected particles ($2 \times 35,108 = 70,216$ gm) is equivalent to 1120 particles or 4714 lbs per foot of tube. Figure 2b shows the height of the tube neck versus time. At times in excess of 7 sec, the tube ceases to rise above the height of 3.97 ft. At this time, the average tension force in the membrane becomes stable at approximately 30 lbs per inch (of length of tube) as shown in Figure 2c. Additional evidence that the tube will not accept the injection of any more particles is shown in Figure 2d, which is a plot of the average of the absolute value of all particle velocities versus time. The figure clearly shows that motion has ceased.

8. Three other simulations were made. Photo 17 shows the result for a simulation similar to the previous, except the "pump" head was set to 15 ft of head (6.5 psi) which is (probably) more consistent with the actual field dredge pump pressure mentioned in Paragraph 3 (with some pipe friction loss). Figures 3a-3d indicate that (2×49528) or 99056 gm of material (or 1580 particles) were injected; that the tube achieved a height of 5.76 ft; and the tension force generated in the membrane was 62 lbs /in. This simulation as regards the height of tube is in good agreement with field observations.

9. The last two simulations were conducted to determine the effects of the angle of internal friction, ϕ , between the "sand" grains. The tube shape depicted in Photo 18 was the result of specifying a "pump" pressure of 8 ft of water and $\phi = 15^\circ$. Plots of the injected mass

(actually one half of the mass because of the unmodified printing problem), the tube neck height, the average membrane tension force, and the average velocity of the particles, are shown in Figures 4a-4d. Lowering ϕ to 15° caused only a small increase in the tube neck height, membrane tension, and the mass of particles injected. However, lowering ϕ to a very small value ($\phi=0.1^\circ$) did have a pronounced effect on those parameters as seen in Figures 5a-5d. Photo 19 shows the shape of the tube after particle injection had ceased. The results for the various parameters are shown in the table below.

Pump Head	ϕ	Mass Injected	Tube Height	Membrane Force
8 ft	30	70216	3.97 ft	30 lbs/in
15	30	99056	5.76	62
8	15	73000	4.02	37
8	.1	121000	6.73	158

Table 1.

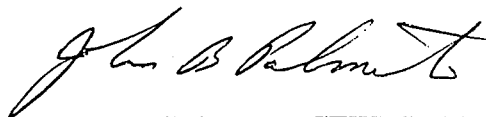
10. Based on these analyses, it appears that as the material becomes more mud-like (i.e., the friction angle decreases) the tube height will increase as will the tension forces in the tube. That is, for a "pump" head of 8 ft, as the friction angle decreased from 30° to 0.1° , the tube height (of a 37 ft circumference tube) increased by 70% (from 3.97 ft to 6.73 ft) and the average tension force increased by 423% (from 30 lbs/in. to 158 lbs/in.). It may be of interest to remark that during the course of these simulations, one was accomplished with ϕ set to zero. During the early stages of that computation, the results appeared to be reasonable. However, during the latter stages of simulation, it appeared that a large portion of the mass gained quite sizable velocities and the tension forces soared to large values on the order of 1000 to 1500 lbs/in. At that time, it was felt that the total lack of frictional resistance resulted in a total loss of numeric damping, and the computed results may have been only a manifestation of the code. Whether or not this type of behavior has real meaning for frictionless "mud," is not yet known; however, Mr. Blama remarked that filling tubes with mud often resulted in numerous tube failures. Another observation that may also be of interest is the time required to fill the tubes to the point where no further particles could, at a given "pump" head, be injected. An examination of the photos indicates filling times, depending on the parameters involved, on the order of 5 to 7 sec. Since each simulation represents the filling of a one cm thick cross-section of tube, the simulated time to fill a 200 ft long tube would be on the order of 8 to 12 hours (i.e., time in hours to fill = time of simulation (sec) X 30.48cm/ft X 200ft X 1hr/3600 sec). It is to be expected that the simulation would overestimate the actual (5 hour) time needed to fill the tube since water velocities (which would greatly aid in the transport of the sand) were not considered. However, the distinct element code does provide for the inclusion of water drag forces which would serve to propel the particles. Perhaps a finite element seepage analysis (non-Darcian, if possible) could provide a handle on the seepage forces and flow velocities for various particle configurations during the filling in order to accommodate this physical aspect. Or, a

new numerical modeling technique entitled the Manifold Method of Material Analysis, recently conceived and now under development by my co-worker Gen-hua Shi, would be a powerful means to incorporate solid and fluid phases in a unified model.

11. In paragraph 4, it was mentioned that impermeable tubes have been used to provide for temporary walls and dikes. It was also mentioned that very accurate (almost analytical) computer programs (such as TANK) have been developed to predict either the tension force, T , the excess water pressure, P_o , or the tube circumference, C , provided two of these parameters are given. However, these solutions are predicated on the assumptions that the tube is sitting on a horizontal frictionless base, that the tube is not making contact with anything but its base, and that the excess water pressure be greater than zero. This solution technique provided a means to evaluate the accuracy of the DE code used for the just-discussed simulations. That is, a provision was included in the DE code to apply an internal fluid pressure to the membrane elements. Figure 6 shows the result from the DE code for an excess pressure, P_o , of 15 ft (or 6.5 psi) and a tube circumference of 37 ft. This simulation produced a tension force of 526 lbs/in. (compare to 537 lbs/in. from TANK on Figure 1) and a tube height of 10.70 ft (compared to 10.26 ft). The area of the inflated tube from the distinct element code was 119.39 sq ft (as compared to 106.5 sq ft). These small differences are due to the "stretch" in the membrane. The contact forces between membrane discs are transmitted by mathematical springs located at the contact points. Use of a higher spring stiffness would have limited the "stretch" and improved the comparison between the two computational methods; however, the CPU time to perform the simulation would have increased. Other simulations with differing tube circumferences and applied pressures gave excellent comparisons to the TANK code. These favorable comparisons to membrane theory, even though the assumptions and restrictions of the theory render it inapplicable for many practical applications, were important to provide credence to the accuracy of the distinct element formulation. However, the application of membrane theory is appropriate for simple situations involving impermeable tubes. That is, for single, non-interacting tubes lying on frictionless, horizontal surfaces, the theory is excellent; however, the theory is not nearly adequate for analyzing the situation depicted in Figure 7a. In this example, two large, immovable, circular barriers interact with the inflating tube. The DE code produced the final shape for an excess pressure of 15 ft (6.5 psi). The barriers caused the tension force within the tube to decrease from the unhindered value of 526 lbs/in. to 445 lbs/in. and the tube height to increase from 10.70 ft to 13.3 ft. Figure 7b shows the situation after the excess pressure had been reduced to 3 ft (1.3 psi). This pressure reduction resulted in a tension force value of 100.8 lbs/in. and a tube height of 11.28 ft. A similar analysis for the barriers shown in Figure 8a, yielded a tension force of 355 lbs/in. and a tube height of 13.71 ft (for an excess pressure of 15 ft). Figure 8b shows the effect of permitting the two large barrier elements to rotate about their centroids (the "+" symbols). Allowing this rotation actually caused the tension force to increase by 103 lbs/in. to 458 lbs/in. and the tube height to rise 0.47 ft to 14.18 ft. Even though the friction angle, ϕ , was set to zero, the redistribution of forces to the barrier elements, resulted in the tube's loss of contact with its horizontal base and all vertical support to be transferred to the angled barrier elements. These very simple examples are presented only to demonstrate the potential usefulness of the DE code. The code can be used to provide solutions to much more complicated situations; e.g., the barrier elements could be replaced by collections of other disc and bar shaped

elements to represent a river bank or to represent one or more separate, but interacting geotubes.

12. Later in the evening of 24 May, I had the opportunity to speak with Mr. Blama about some of his experiences and concerns in regard to geotubes. What struck me in particular was the great amount of emphasis on using field experiences and trials to achieve "design" procedures for other applications. Although field experience is extremely valuable, one must be careful to apply the results of the field observations to design concepts unless one also has a good understanding of the involved physical processes. In an announcement of an upcoming workshop on Geotextile Tube Technology and Applications for Wetlands and Other Habitat Restoration and Protection Projects, Dr. Landin stated *"Each geotextile tube application has resulted in specific questions related to both engineering and environmental techniques and strategies. Furthermore, we do not yet have a predictive capability for tubes."* I am convinced that DE modeling offers an excellent and viable means to provide predictive capabilities for many geotextile tube applications. To date, the two applications which I have simulated as a feasibility concept have led to very good agreement with the observations. Proposals to develop and test DE schemes have been prepared and forwarded to various WES program managers, and I remain hopeful that funding from those involved with obtaining solutions to geotextile tube problems will soon be obtained.



John B. Palmerton CEWES-GS-R
Research Civil Engineer
Soil and Rock Mechanics Division, GL
(601) 634-3357

CF:

CEWES-ZB/COL Howard
CEWES-GV-Z/Marcuson
CEWES-GS-S/Gilbert
CEWES-CP-D/McNair
CEWES-CD-SE/Clausner
CEWES-CD-SE/Davis
CEWES-ER-W/Landin
CEWES-EP-D/Patin
CENAB/Blama



Photo 1.

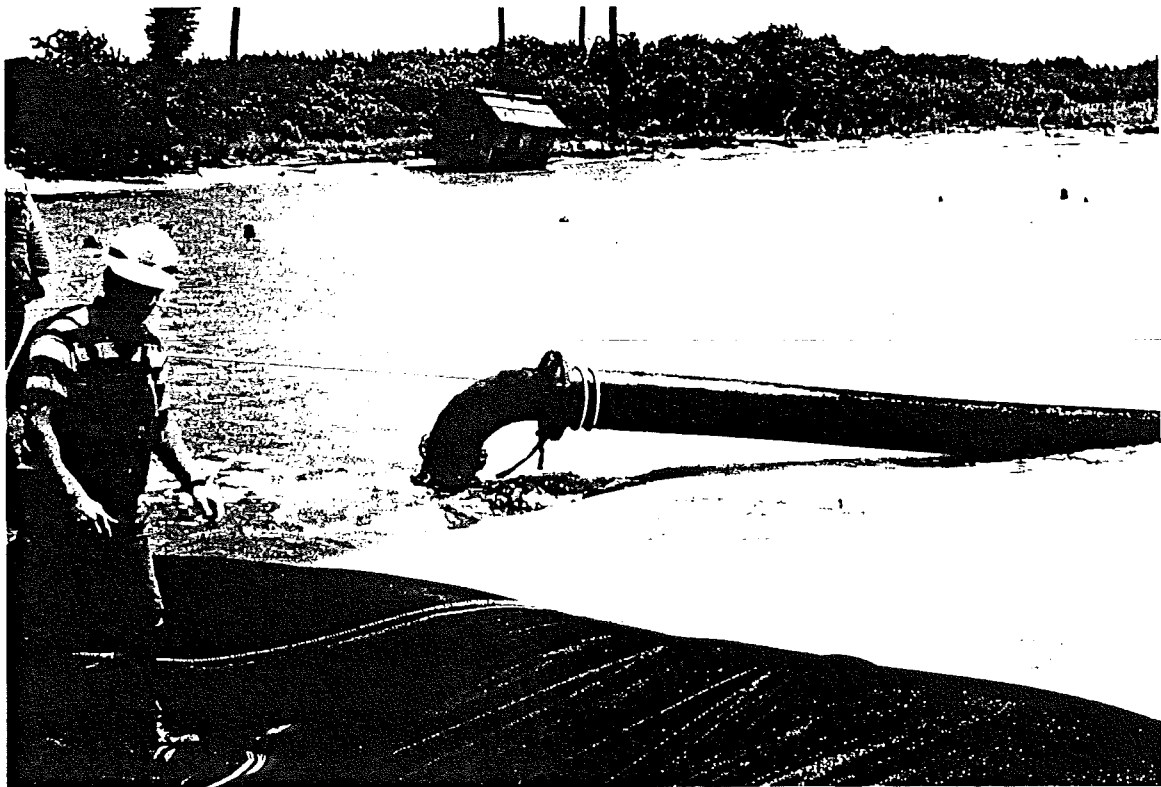


Photo 2.

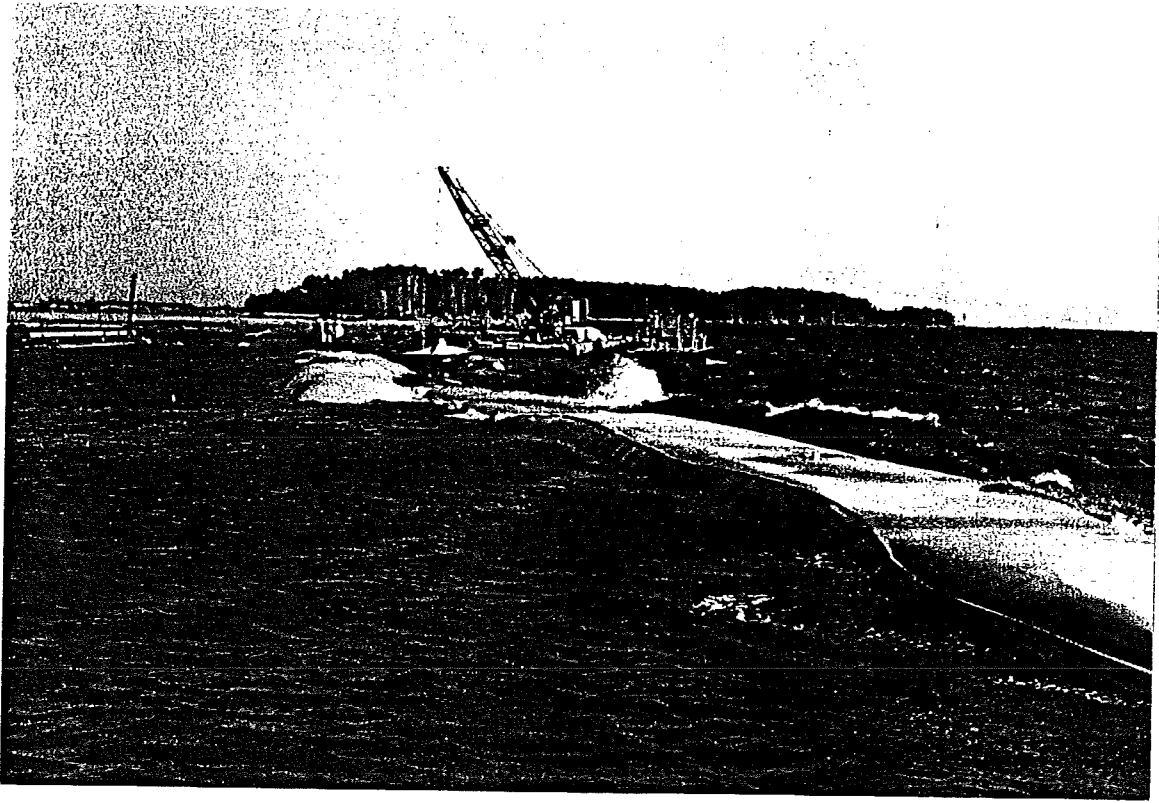


Photo 3.

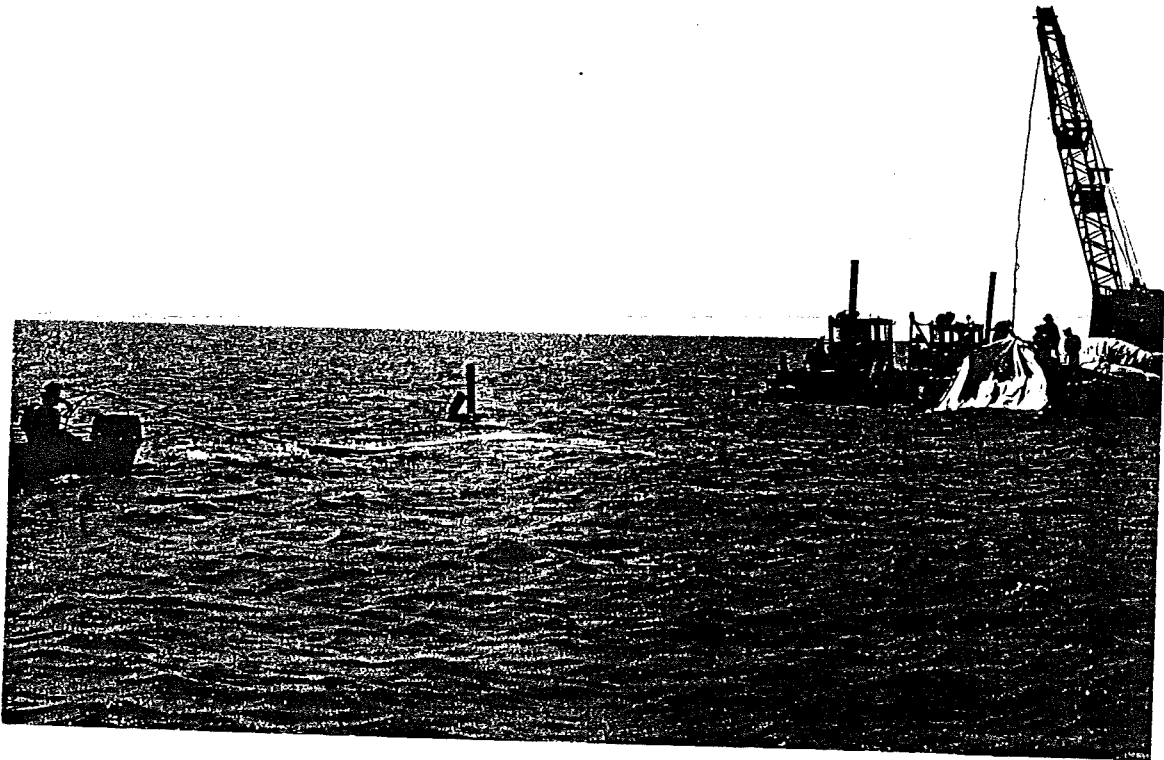


Photo 4.

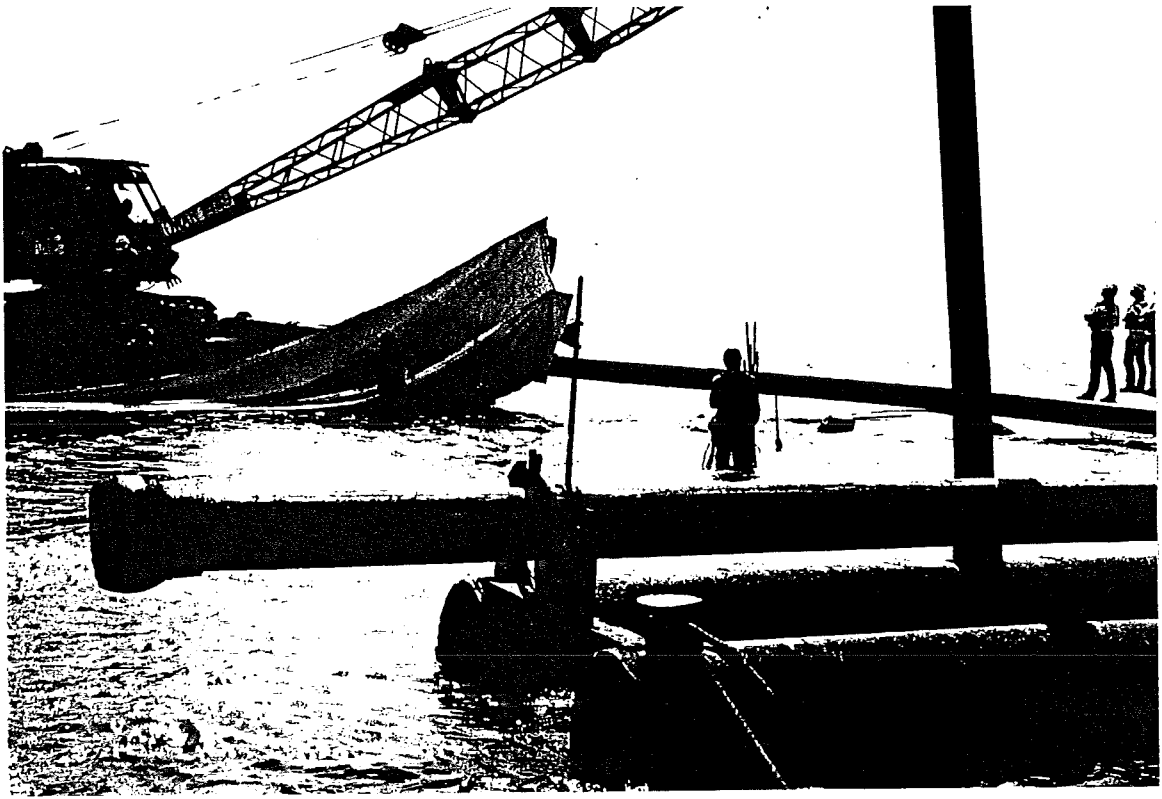


Photo 5.

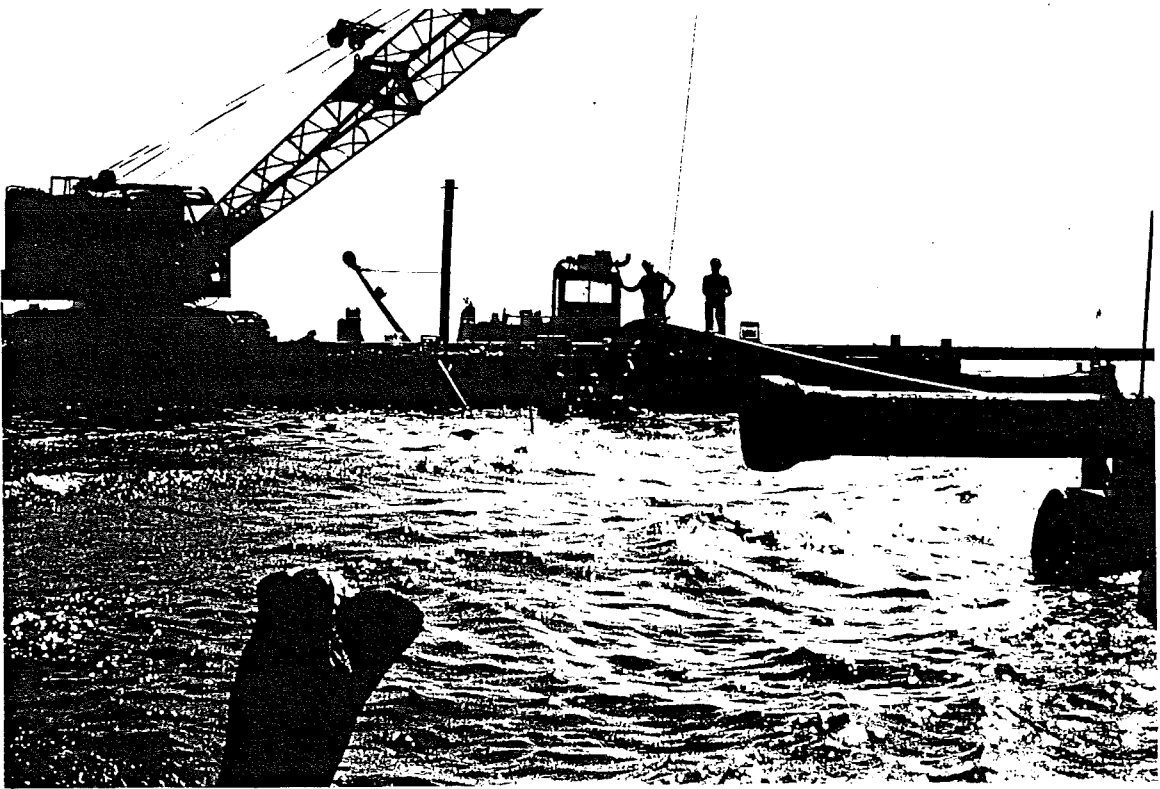


Photo 6.

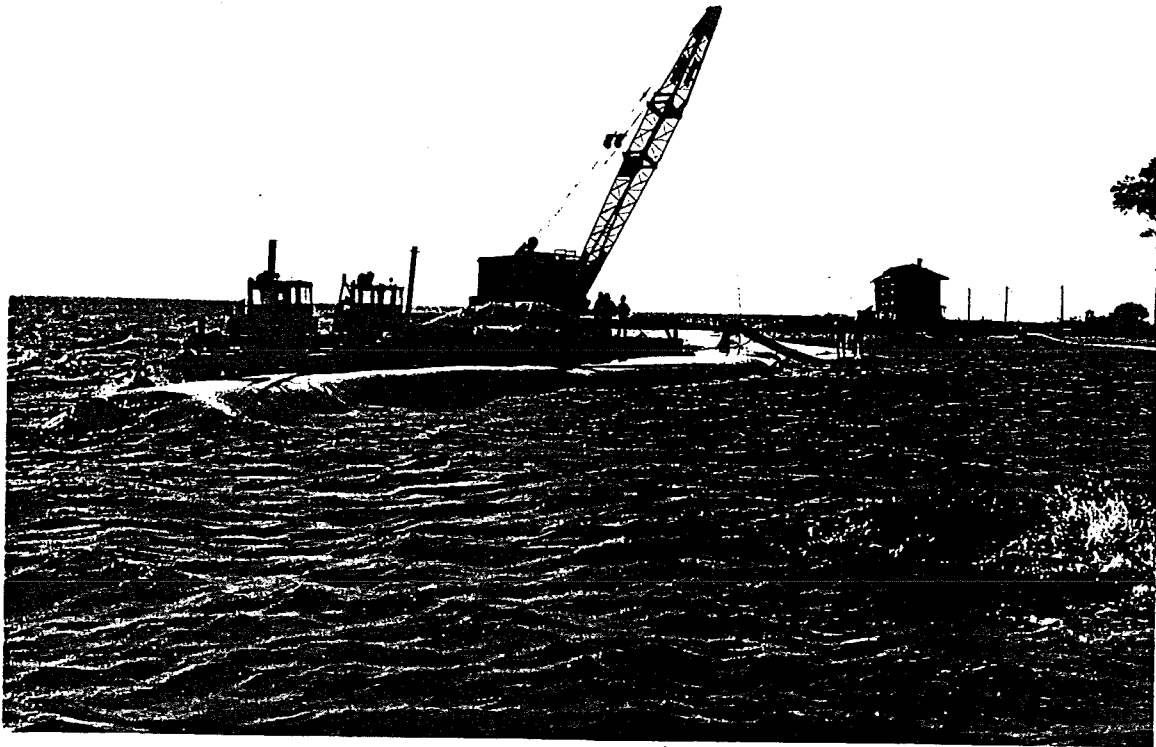


Photo 7.

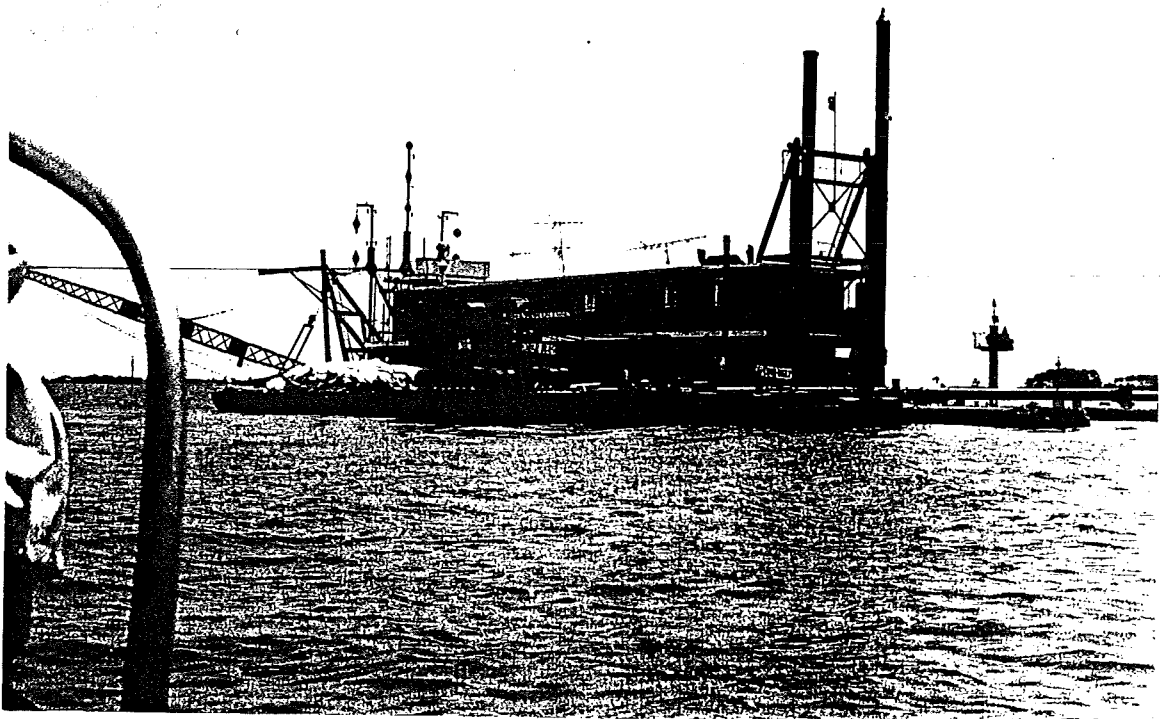


Photo 8.

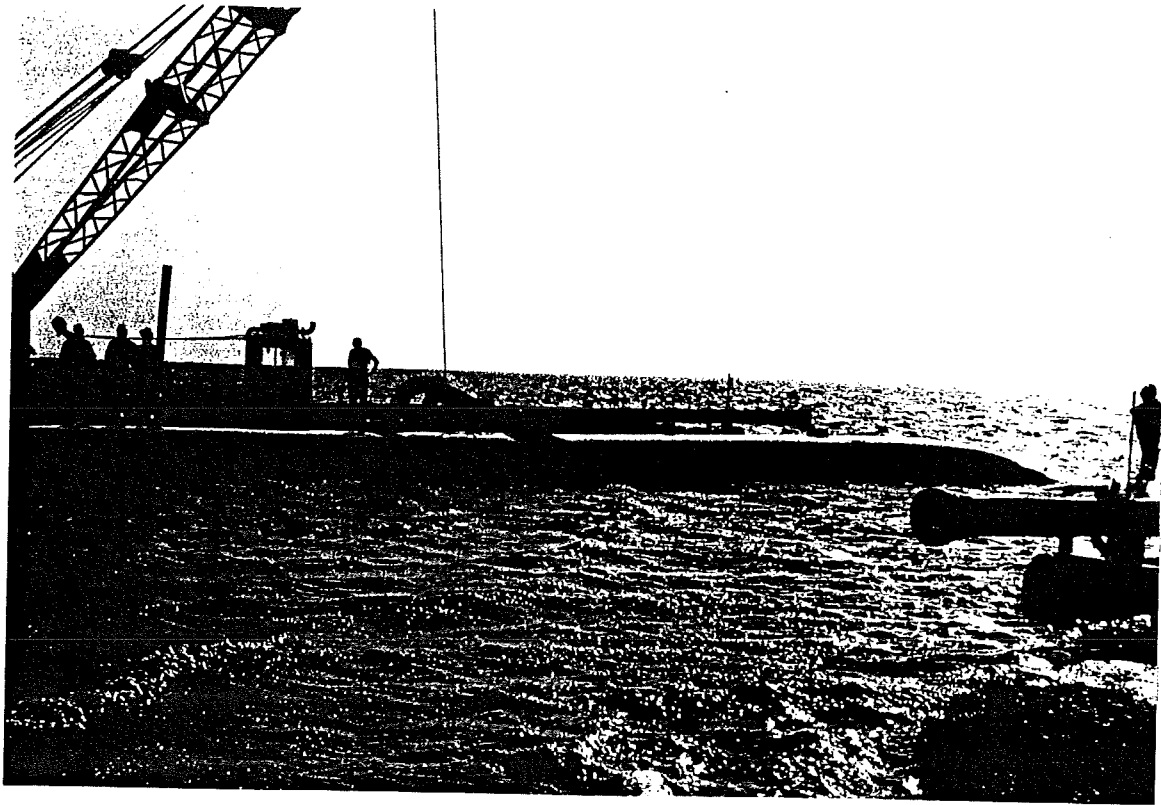


Photo 9.

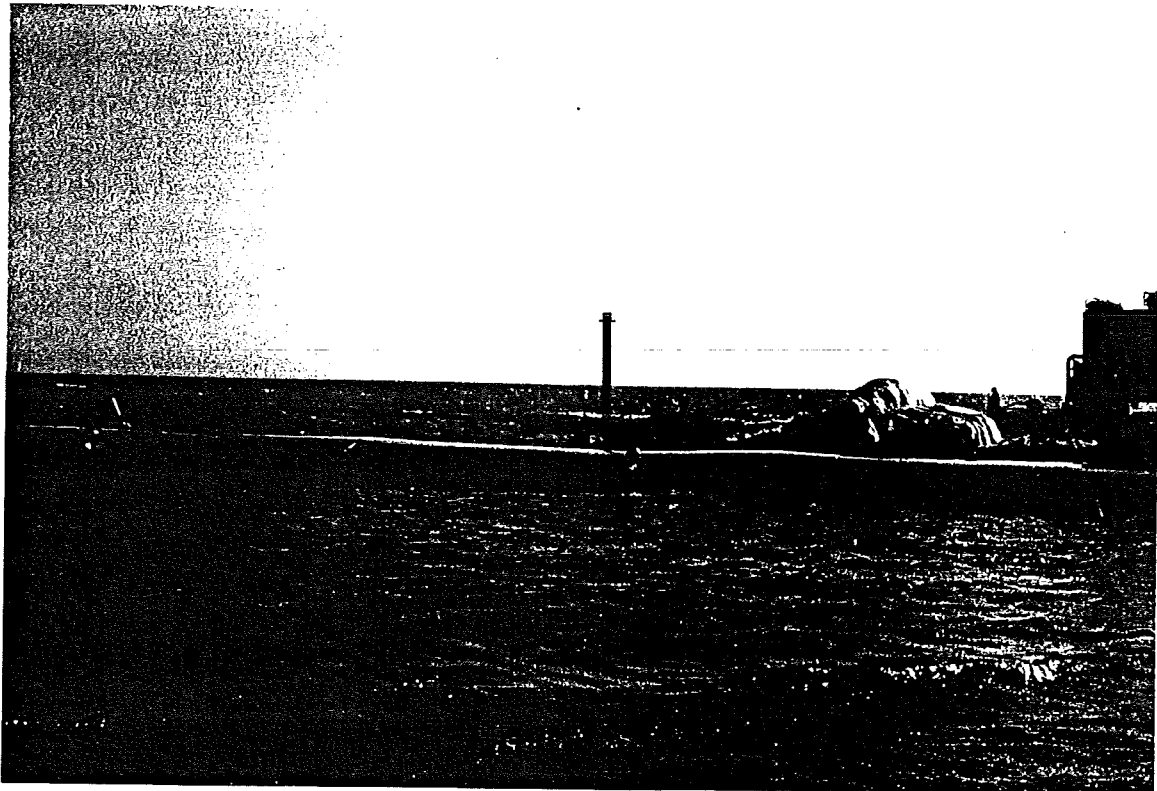
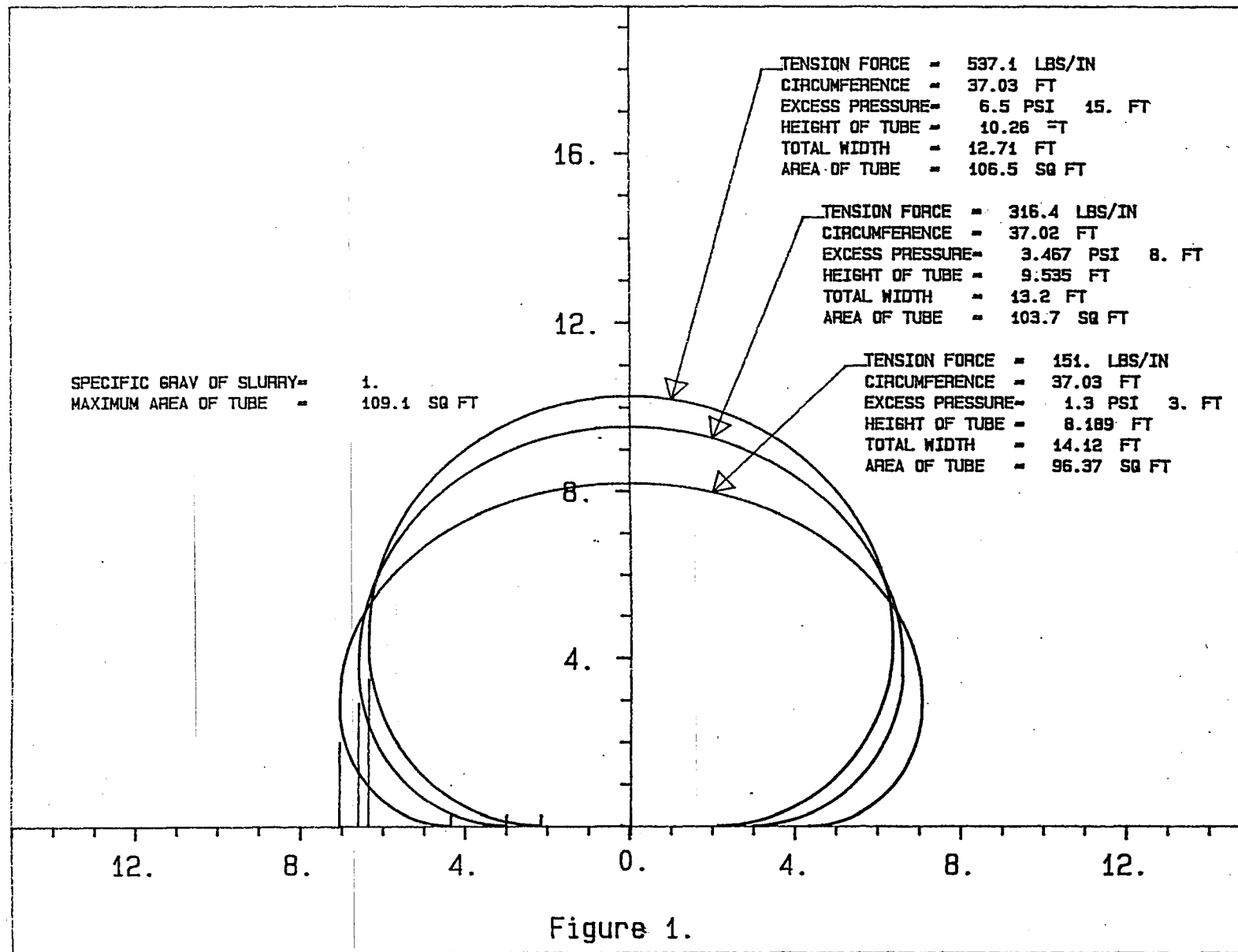


Photo 10.



```

*****
GIVEN P=15 ft    C=37 ft
  DENSITY OF SLURRY =      62.40 pcf
    SPG OF SLURRY =       1.00
  TOTAL TUBE CIRCUMFERENCE = 37.03 ft
  EXCESS PRESSURE -TOP OF TUBE = 6.50 psi      15.00 ft
    TENSION FORCE IN TUBE = 6445.06 lbs/ft    537.09 lbs/inch
    TOTAL HEIGHT OF TUBE = 10.26 ft
    TOTAL WIDTH OF TUBE = 12.71 ft
    FLAT BASE WIDTH OF TUBE = 4.24 ft
  CROSS-SECTIONAL AREA OF TUBE = 106.48 sq ft    97.58 % OF CAPACITY
    BASE PRESSURE = 1576.48 psf
    = 10.95 psi
    = 25.26 ft (water)

```

```

*****
GIVEN P=8 ft    C=37 ft
  DENSITY OF SLURRY =      62.40 pcf
    SPG OF SLURRY =       1.00
  TOTAL TUBE CIRCUMFERENCE = 37.02 ft
  EXCESS PRESSURE -TOP OF TUBE = 3.47 psi      8.00 ft
    TENSION FORCE IN TUBE = 3796.22 lbs/ft    316.35 lbs/inch
    TOTAL HEIGHT OF TUBE = 9.53 ft
    TOTAL WIDTH OF TUBE = 13.20 ft
    FLAT BASE WIDTH OF TUBE = 5.94 ft
  CROSS-SECTIONAL AREA OF TUBE = 103.67 sq ft    95.04 % OF CAPACITY
    BASE PRESSURE = 1094.15 psf
    = 7.60 psi
    = 17.53 ft (water)

```

```

*****
GIVEN P=3 ft    C=37 ft
  DENSITY OF SLURRY =      62.40 pcf
    SPG OF SLURRY =       1.00
  TOTAL TUBE CIRCUMFERENCE = 37.03 ft
  EXCESS PRESSURE -TOP OF TUBE = 1.30 psi      3.00 ft
    TENSION FORCE IN TUBE = 1811.46 lbs/ft    150.95 lbs/inch
    TOTAL HEIGHT OF TUBE = 8.19 ft
    TOTAL WIDTH OF TUBE = 14.12 ft
    FLAT BASE WIDTH OF TUBE = 8.63 ft
  CROSS-SECTIONAL AREA OF TUBE = 96.37 sq ft    88.33 % OF CAPACITY
    BASE PRESSURE = 698.22 psf
    = 4.85 psi
    = 11.19 ft (water)

```

Figure 1 (cont).

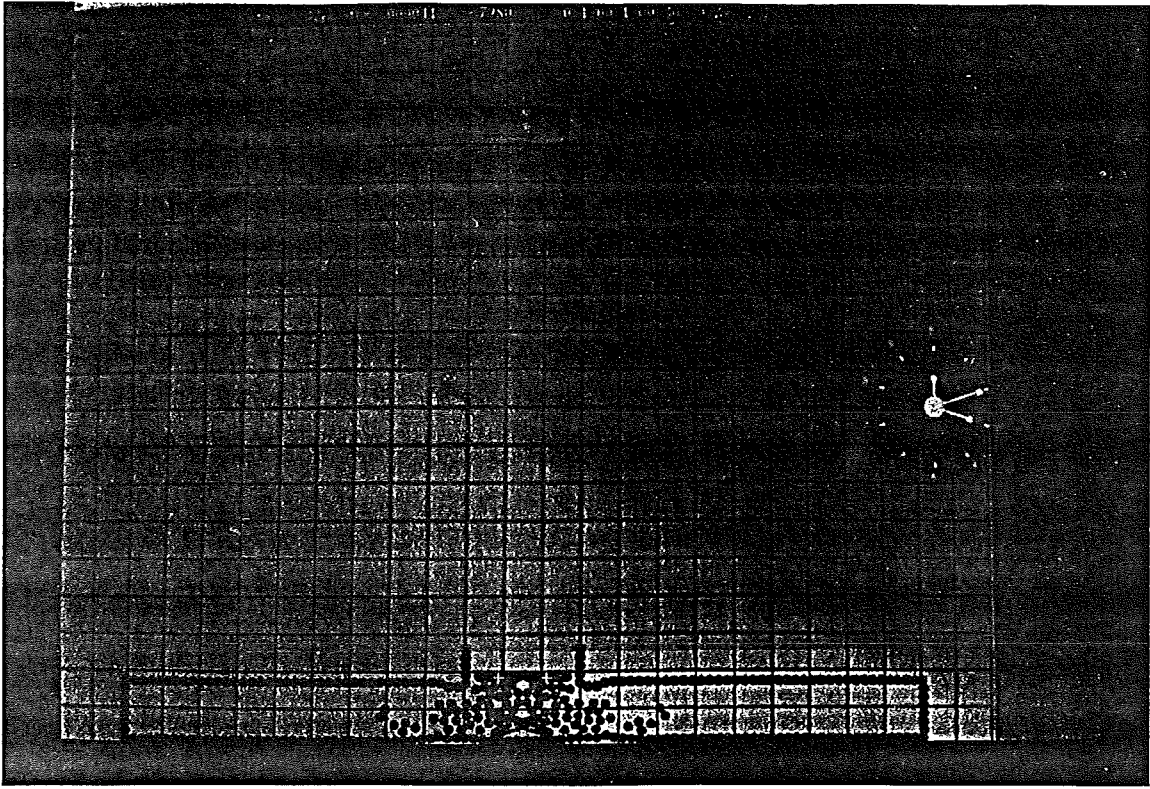


Photo 11.

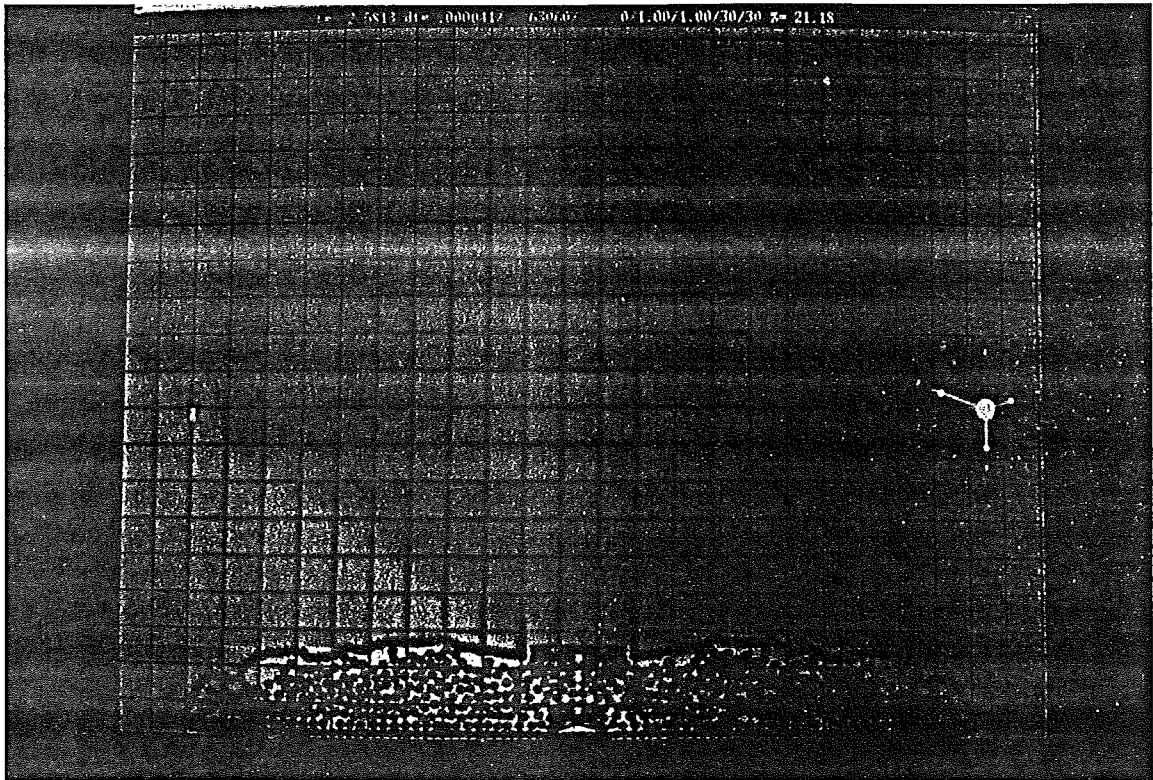


Photo 12.

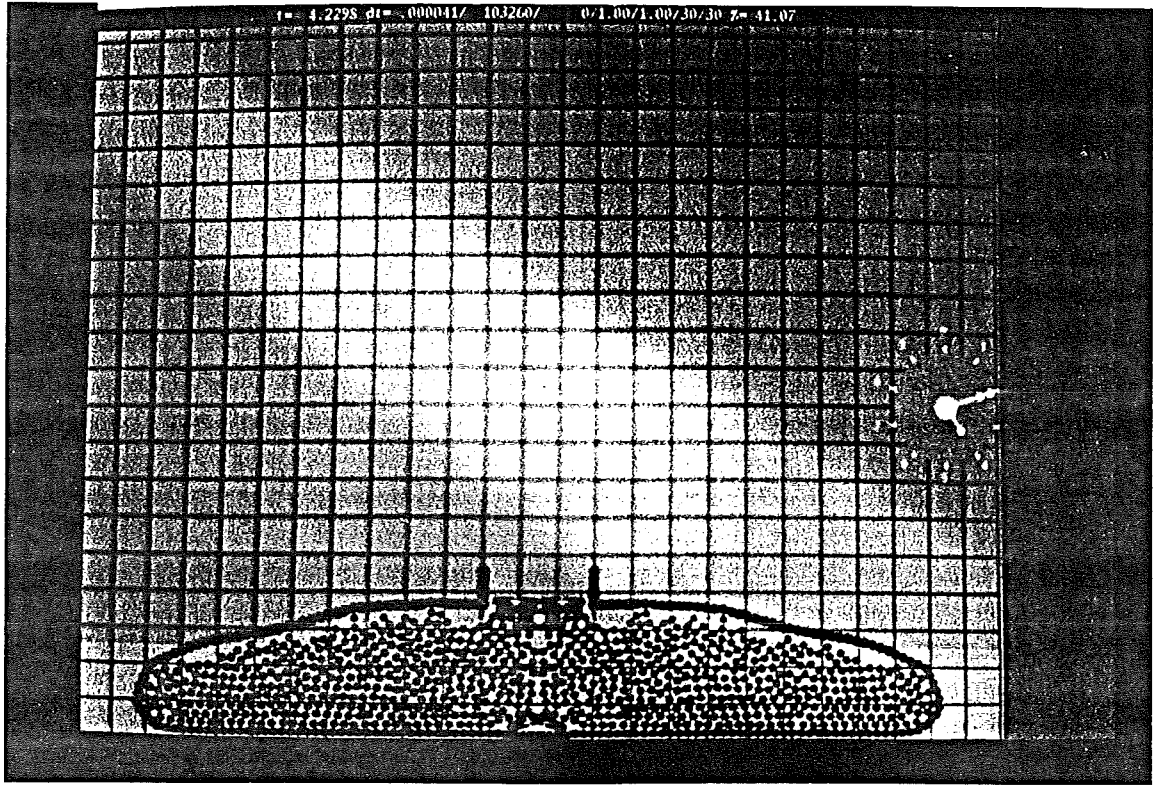


Photo 13.

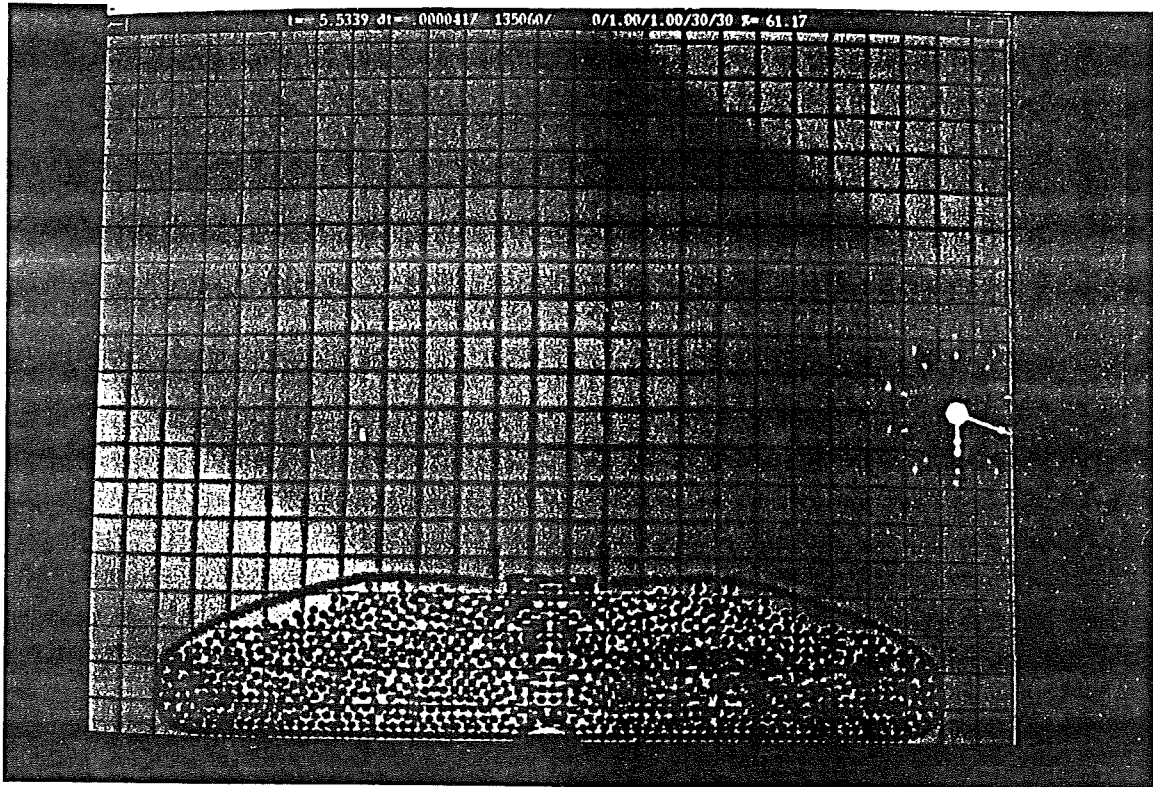


Photo 14.

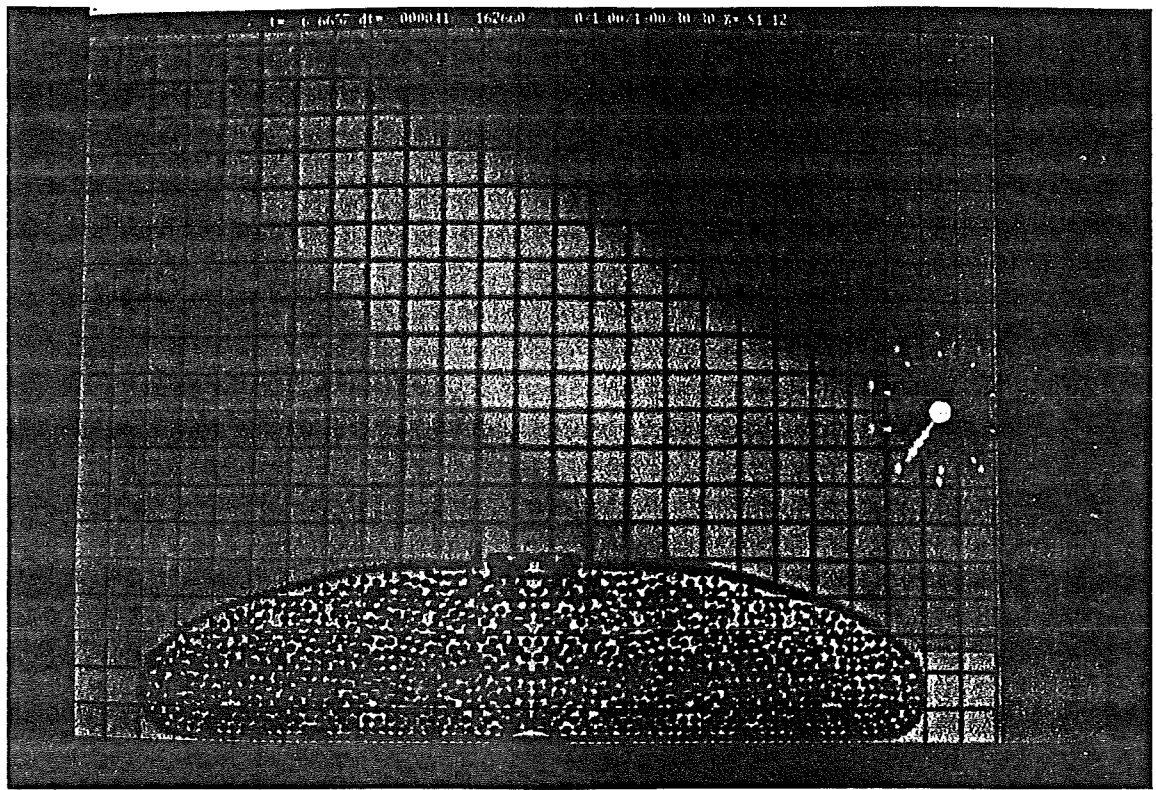


Photo 15.

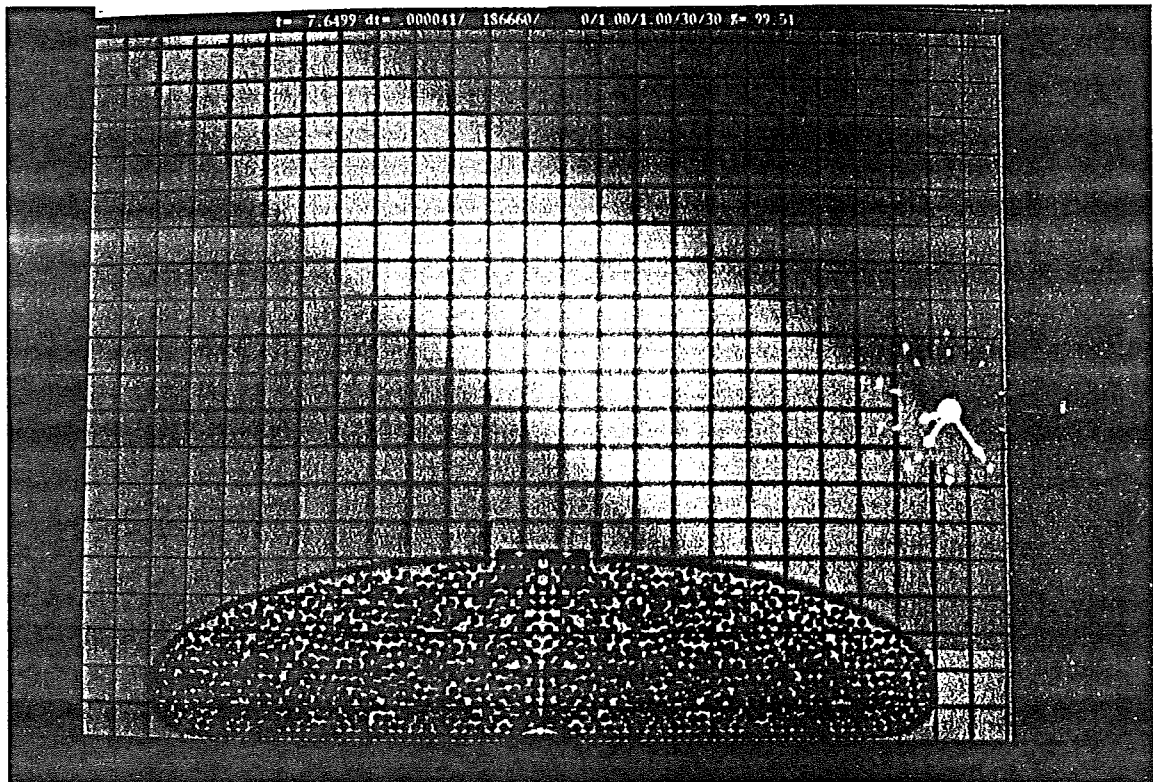


Photo 16.

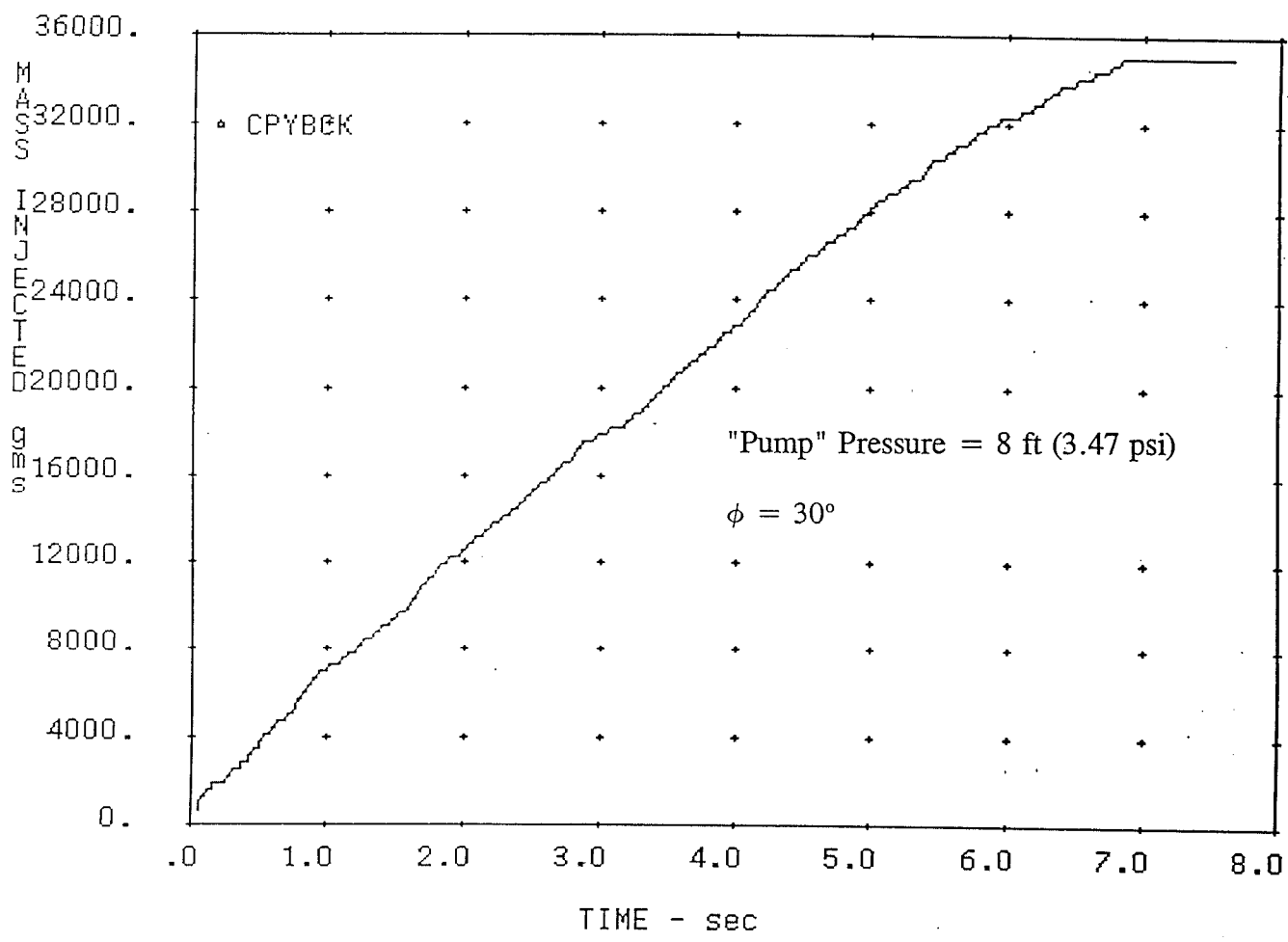


Figure 2a.

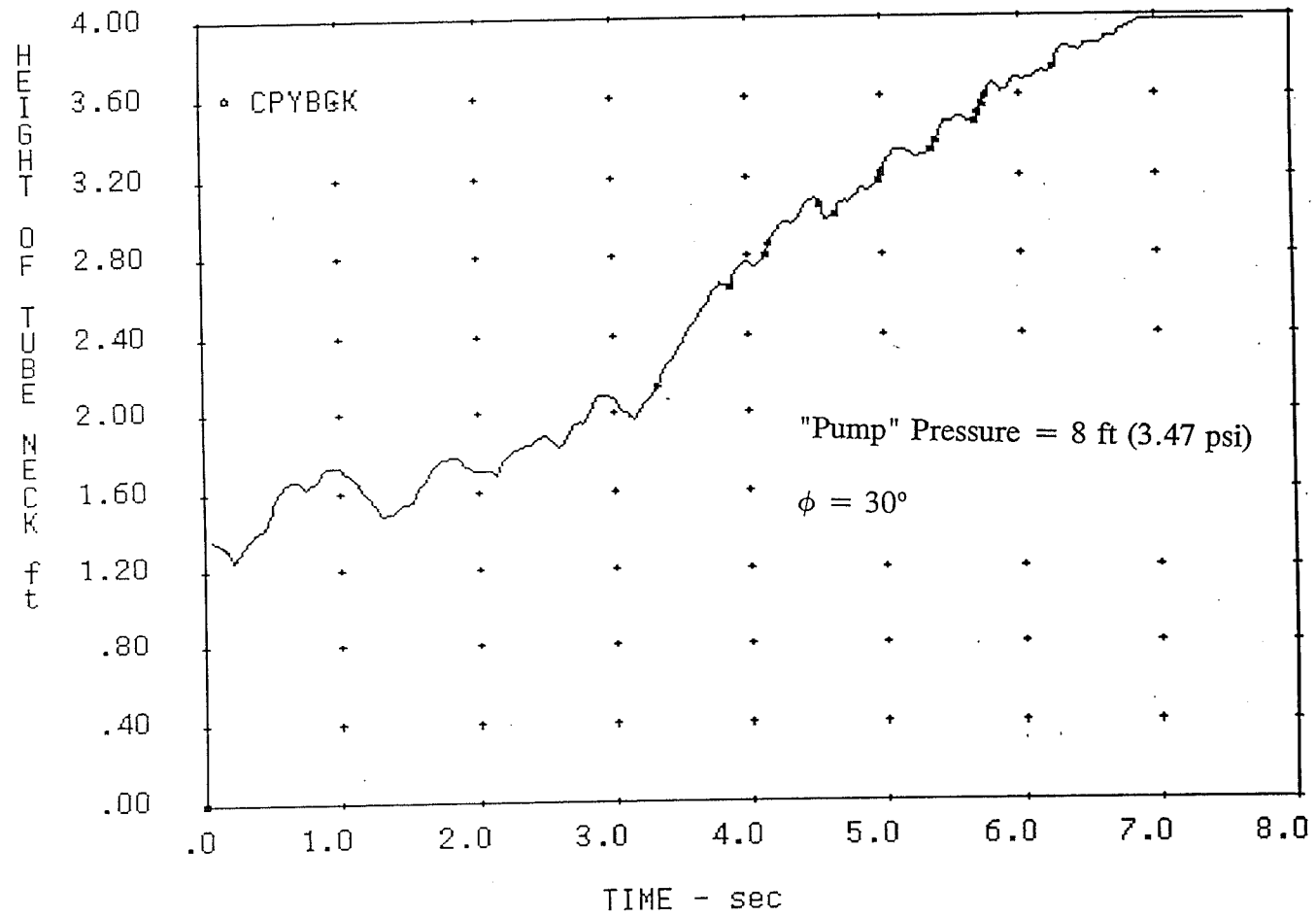


Figure 2b.

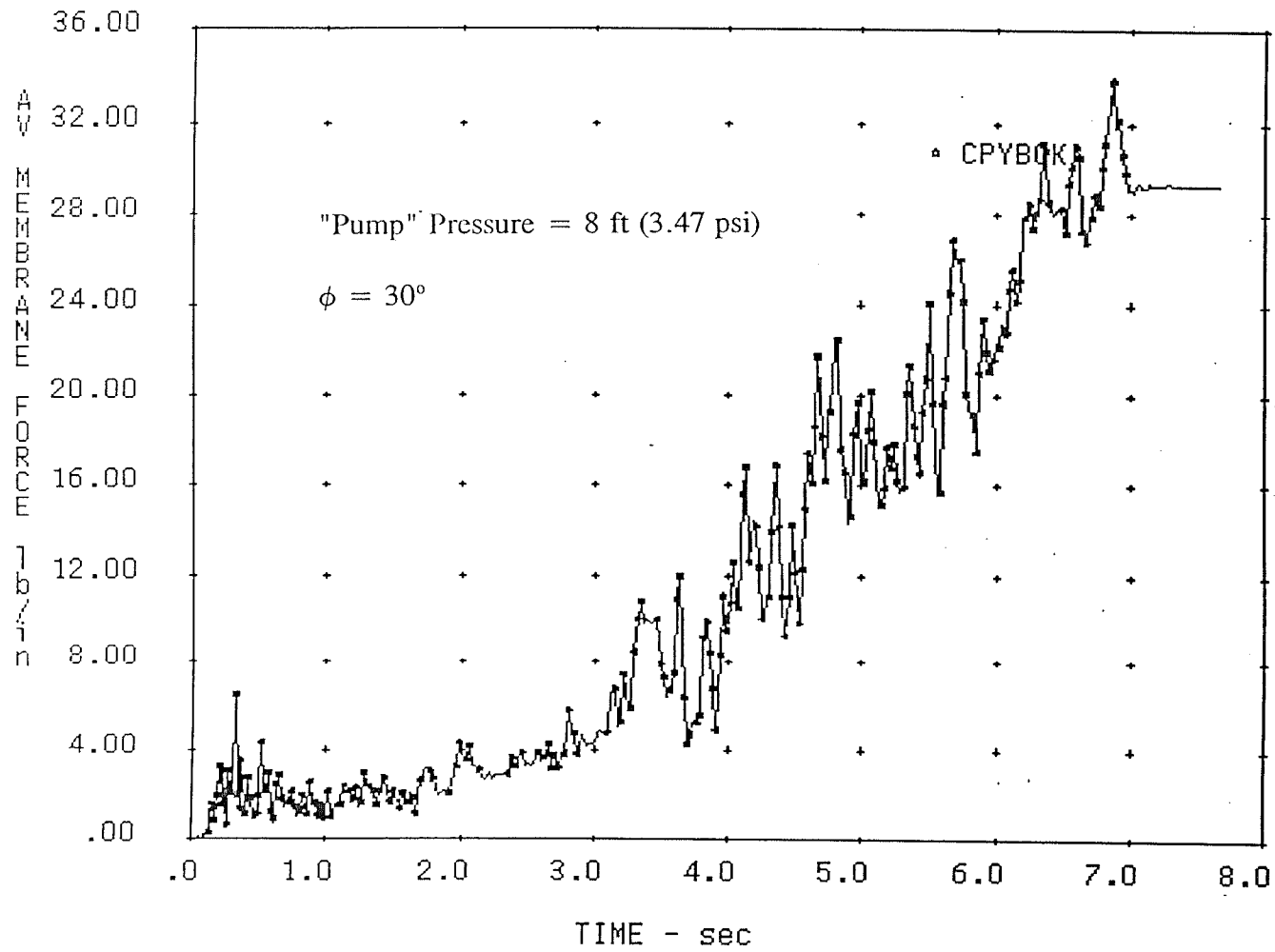


Figure 2c.

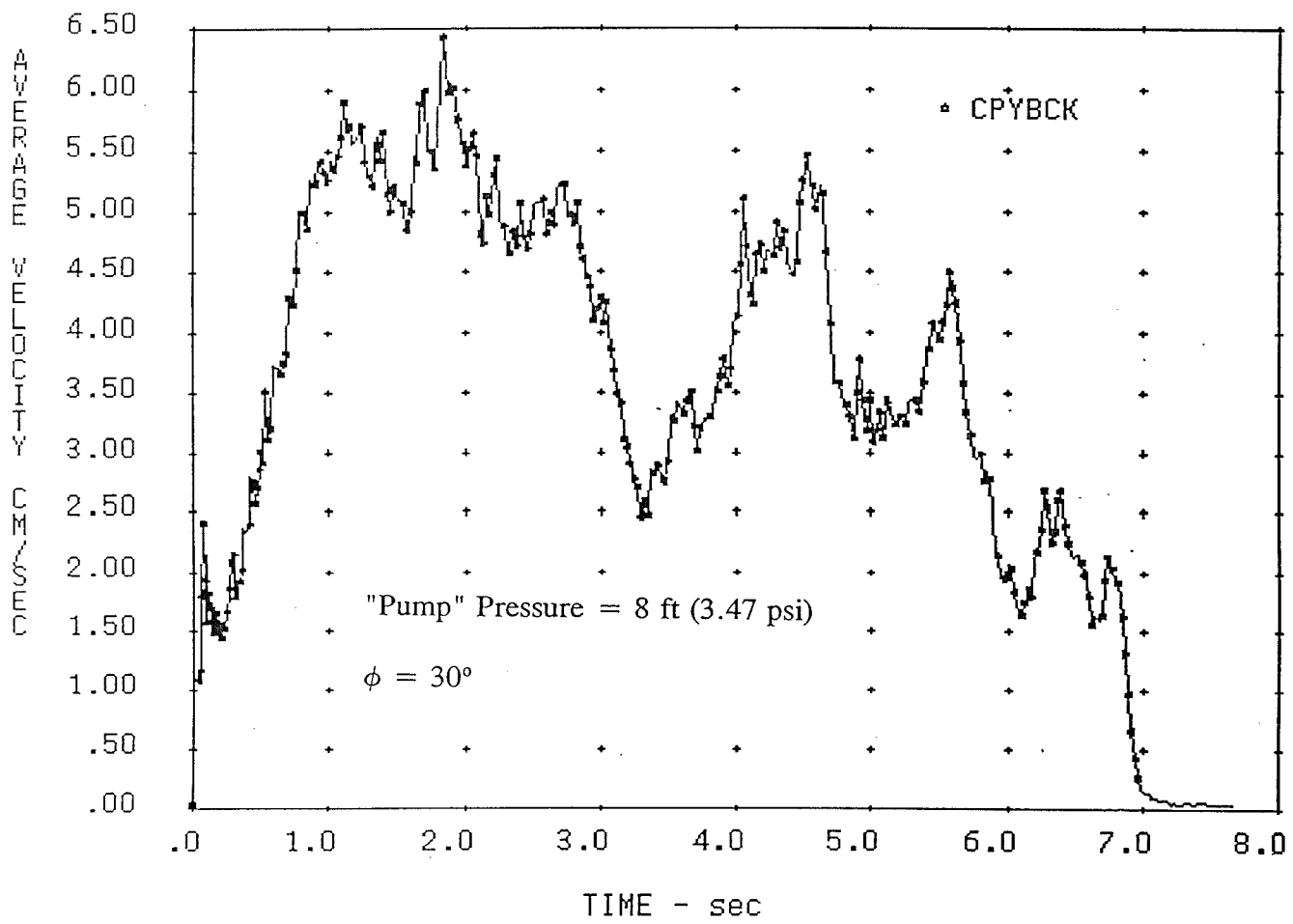


Figure 2d.

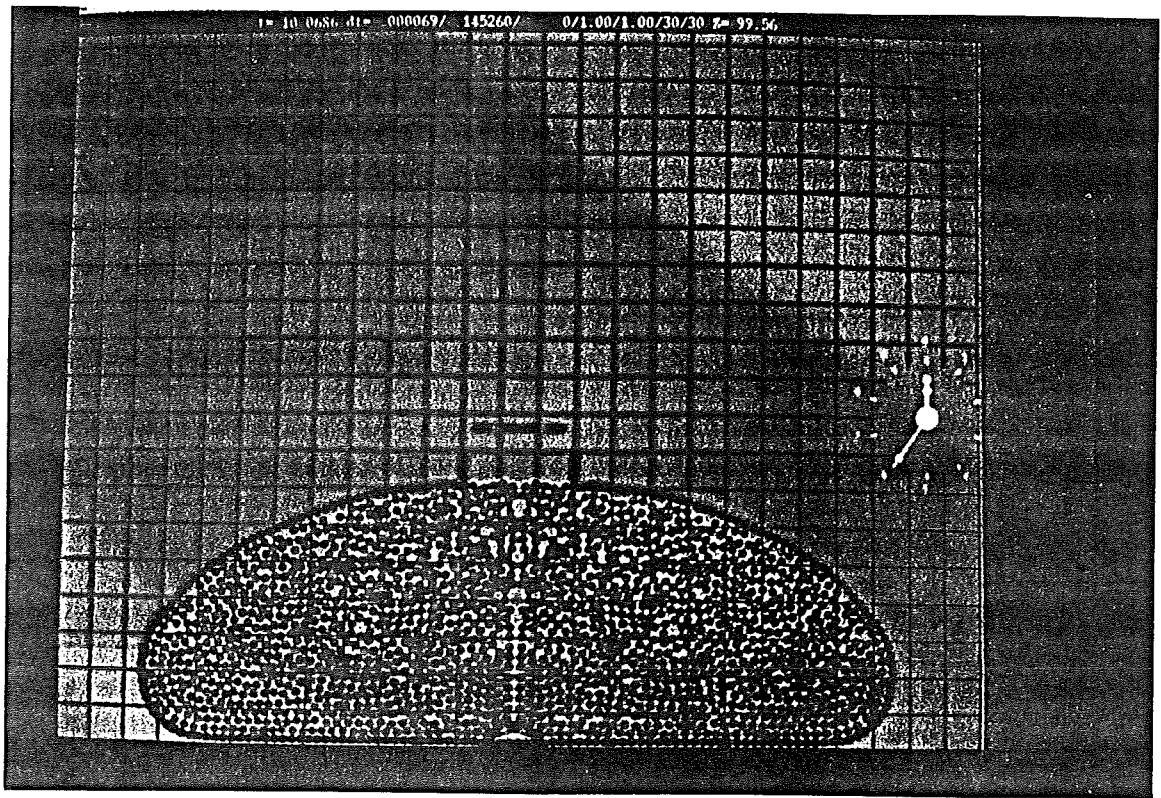


Photo 17.

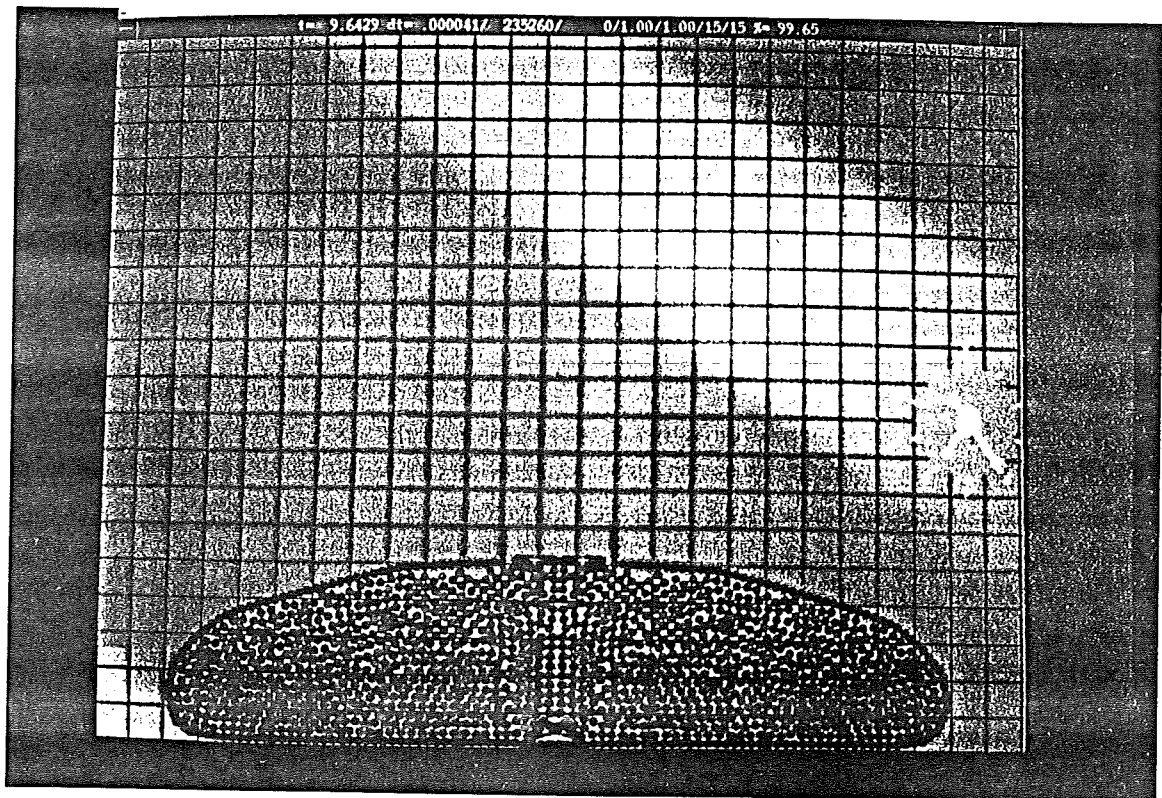


Photo 18.

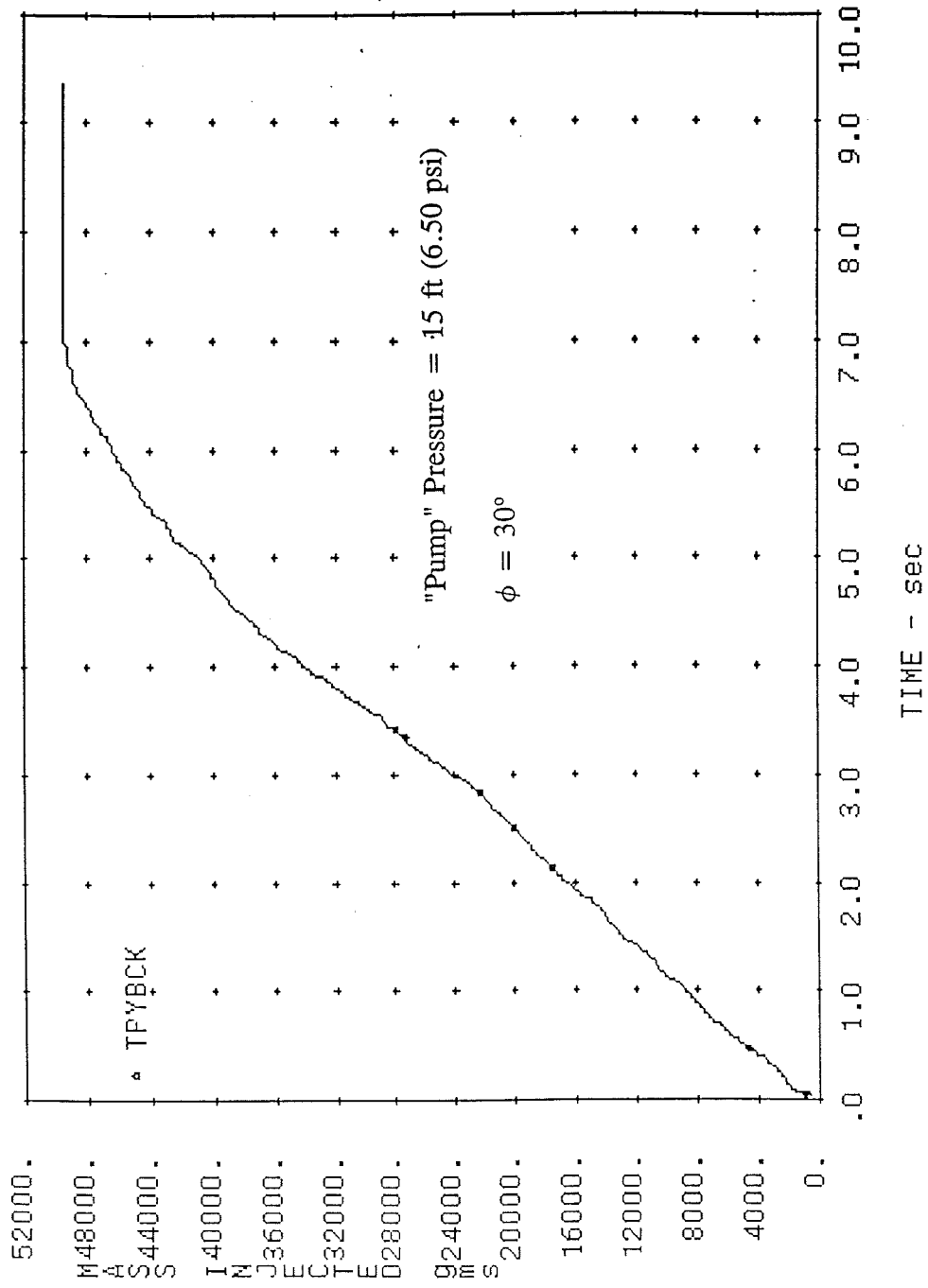


Figure 3a.

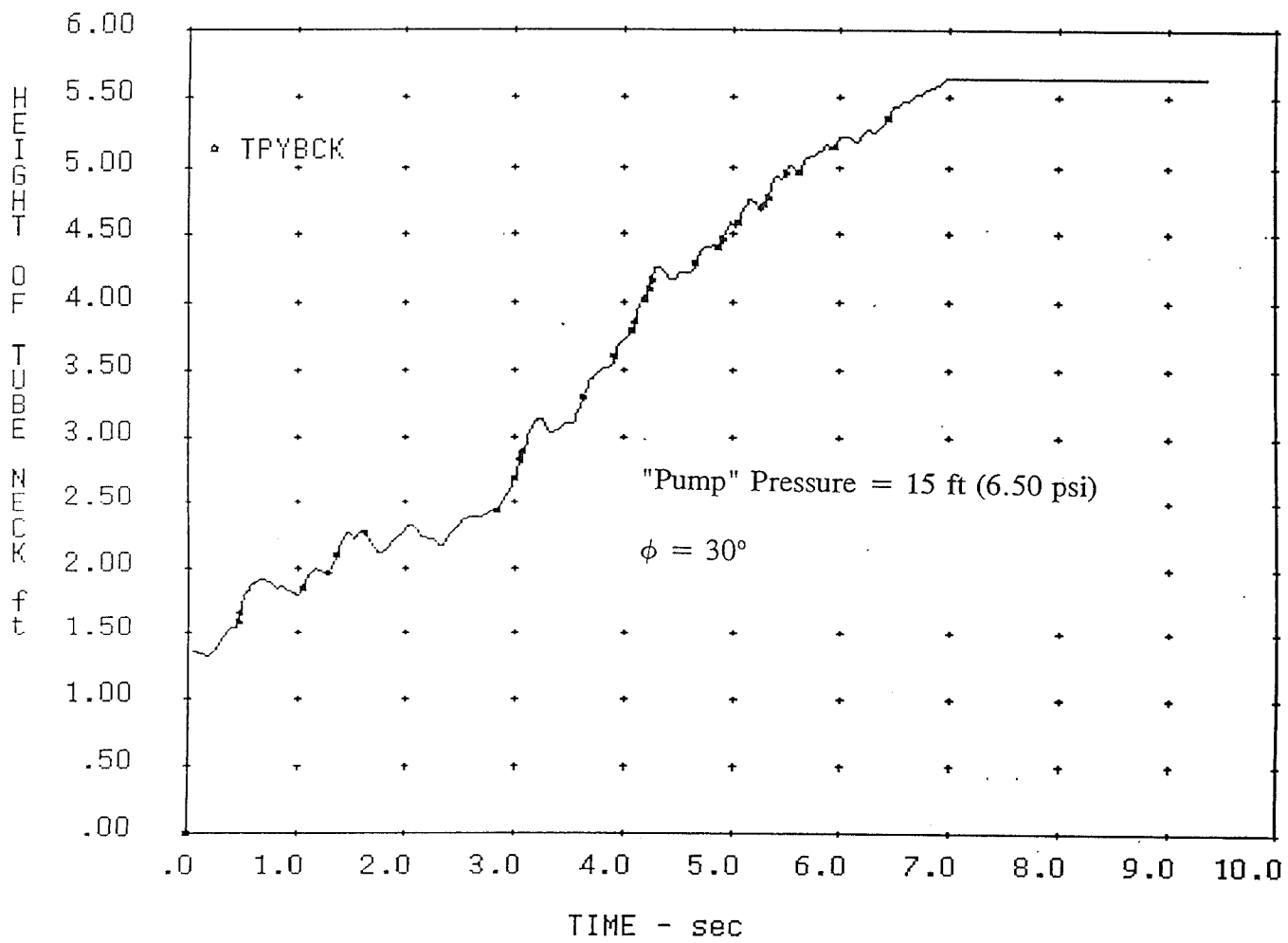


Figure 3b.

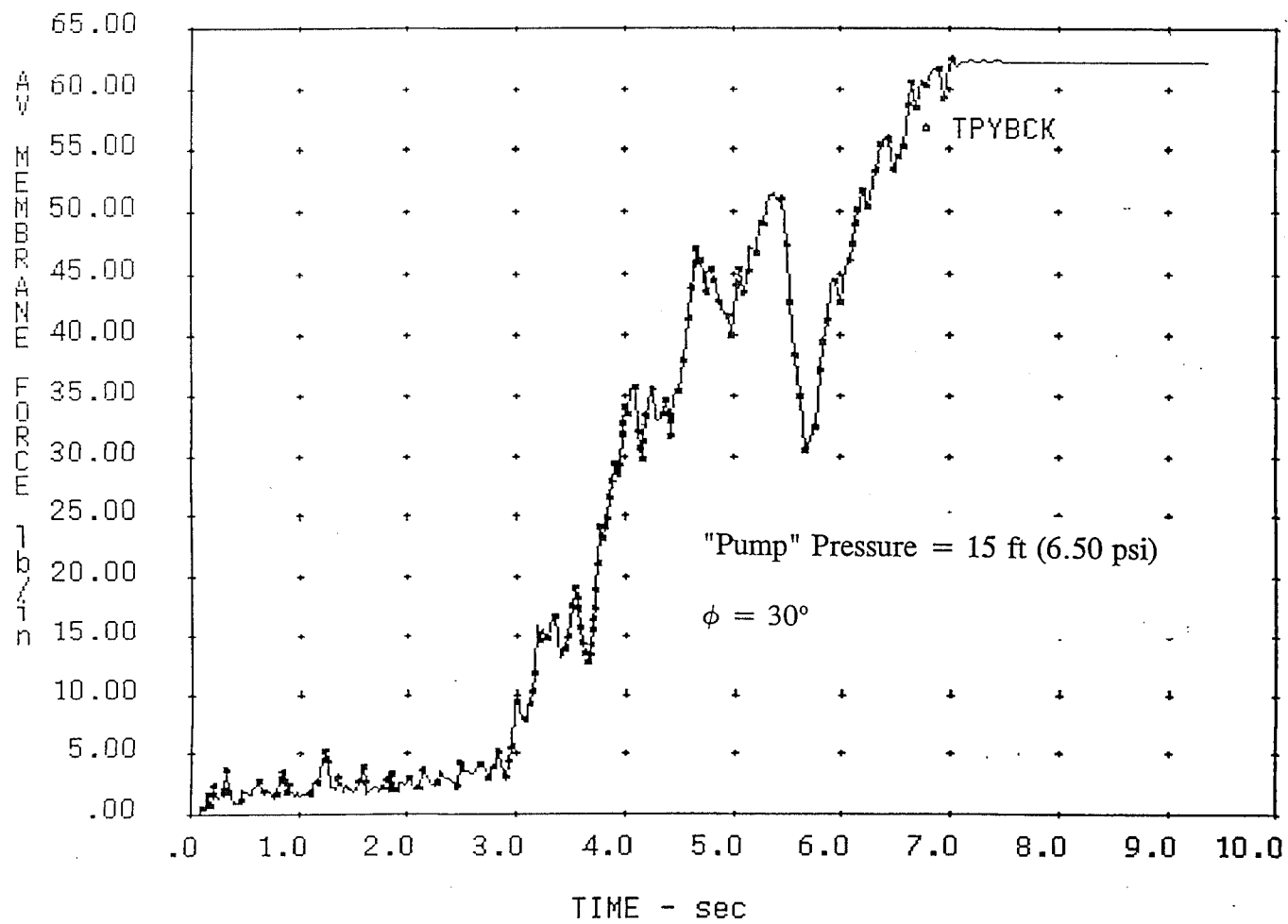


Figure 3c.

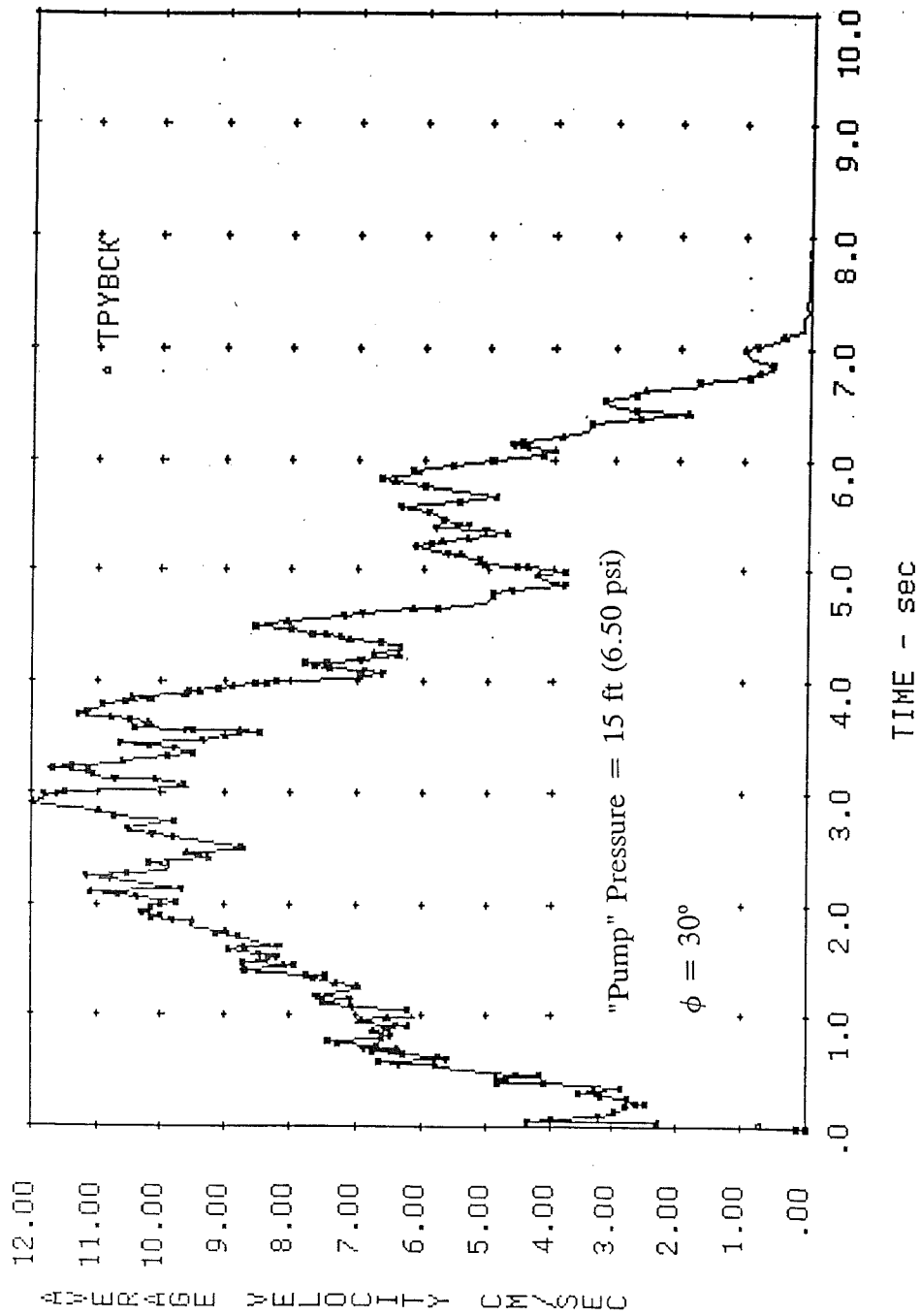


Figure 3d.

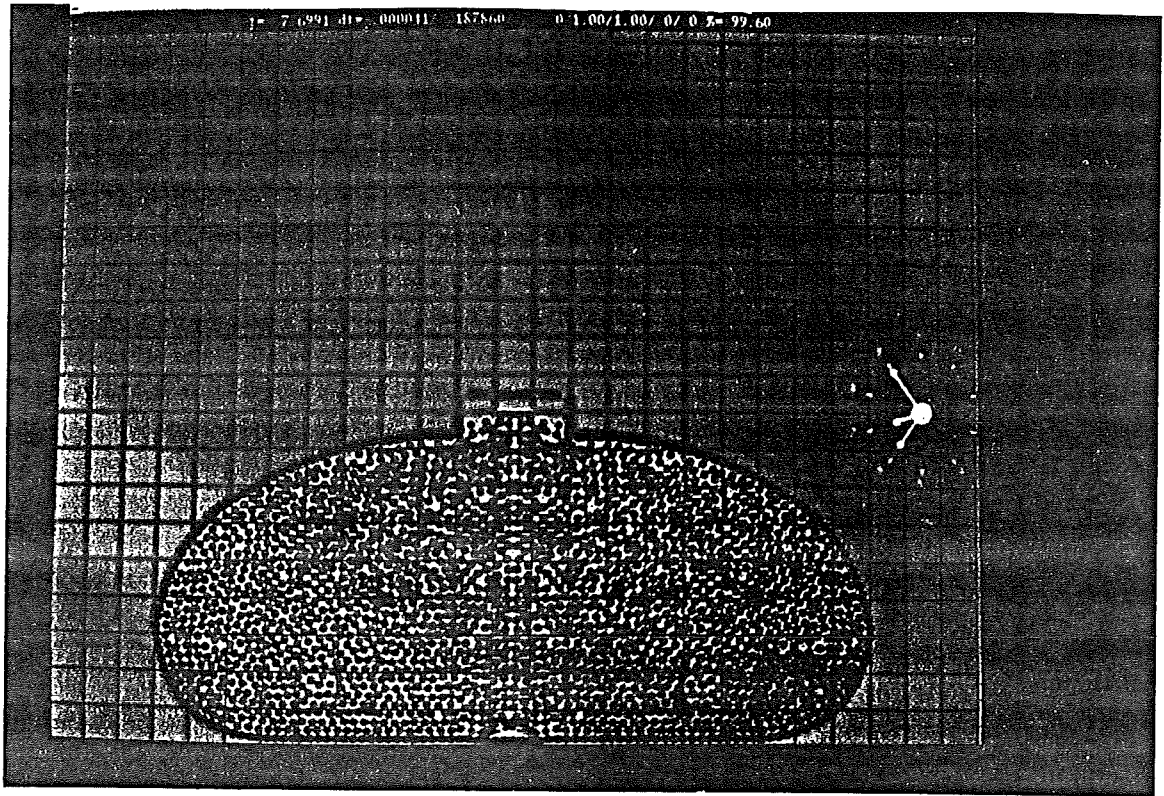


Photo 19.

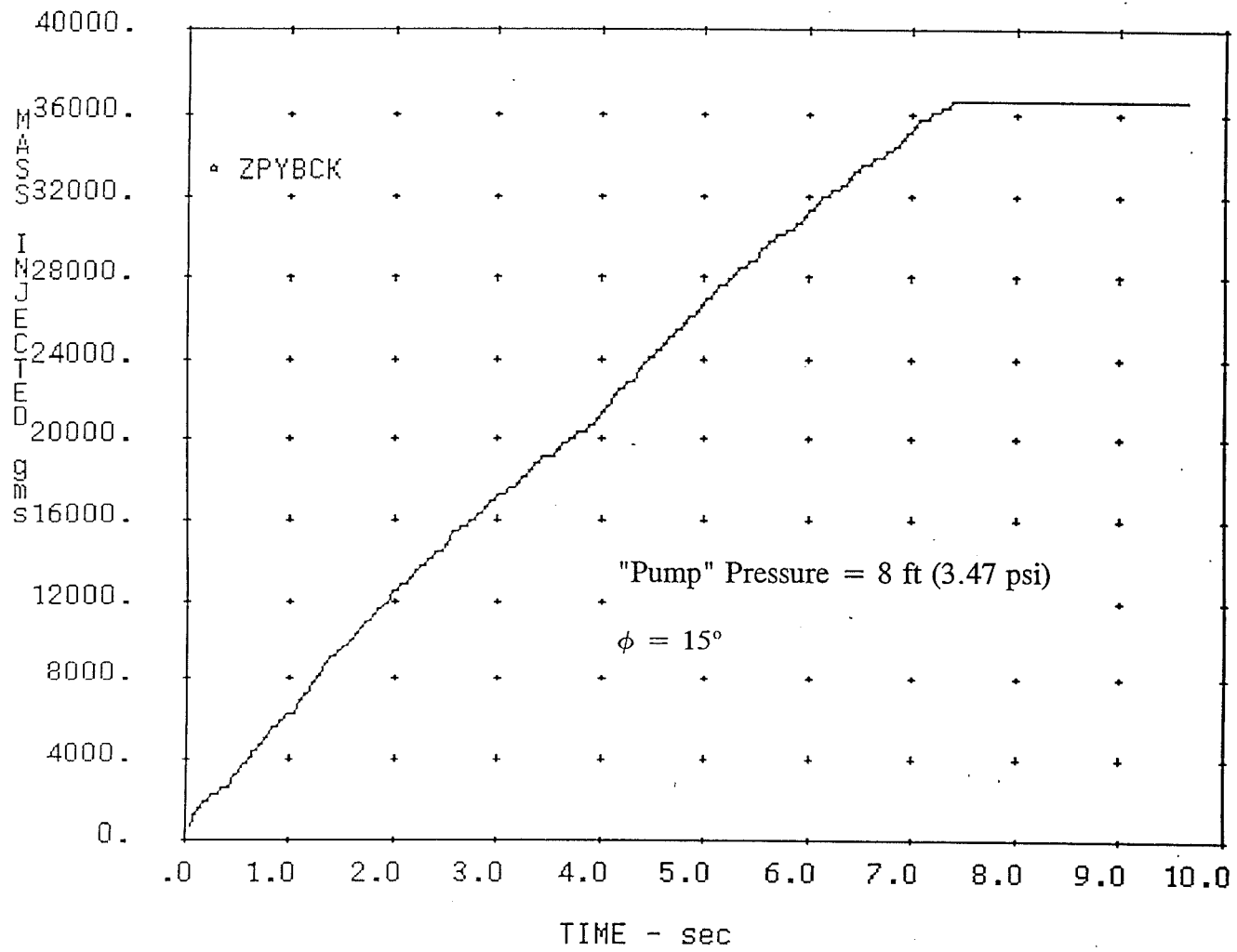


Figure 4a.

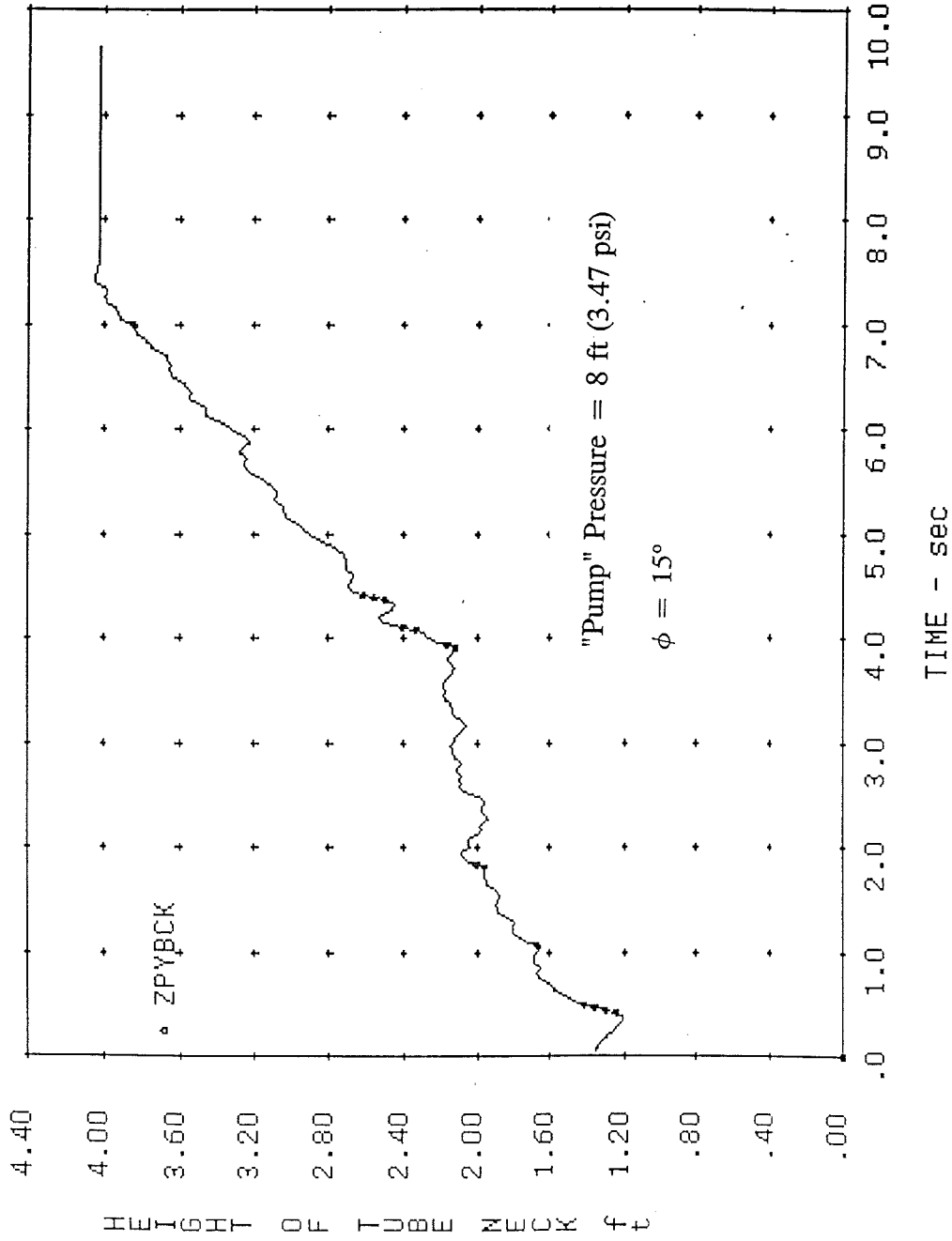


Figure 4b.

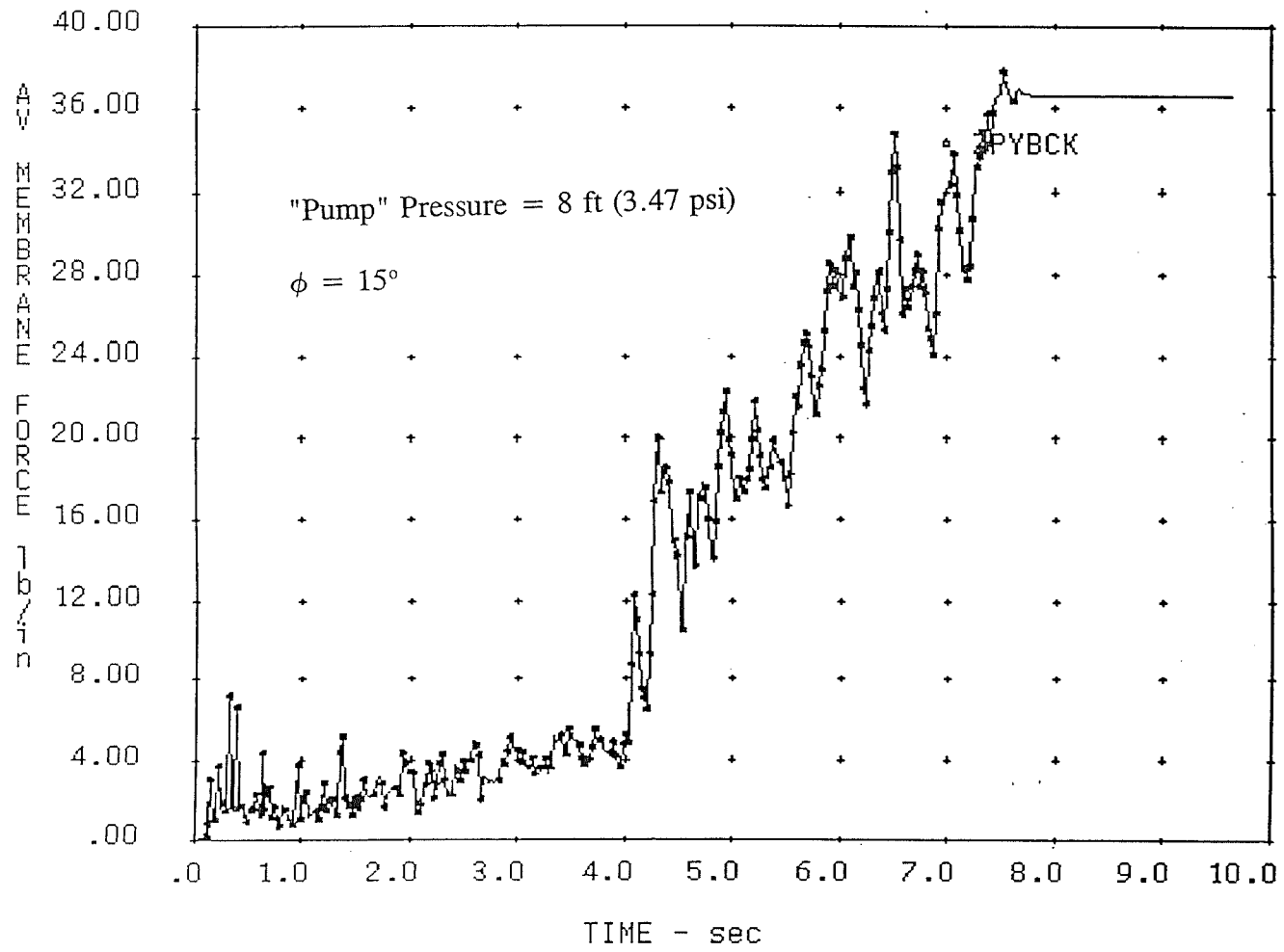


Figure 4c.

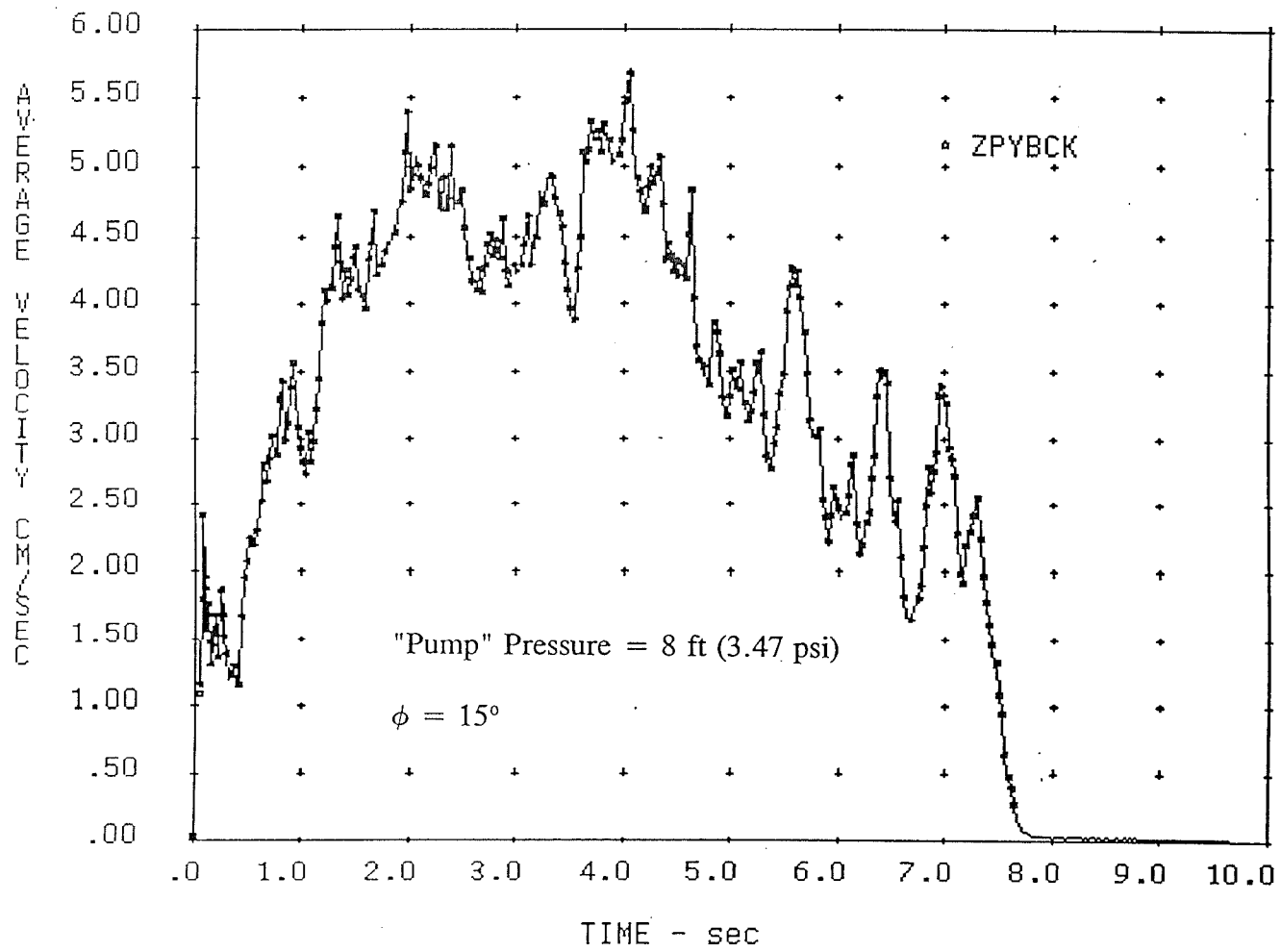


Figure 4d.

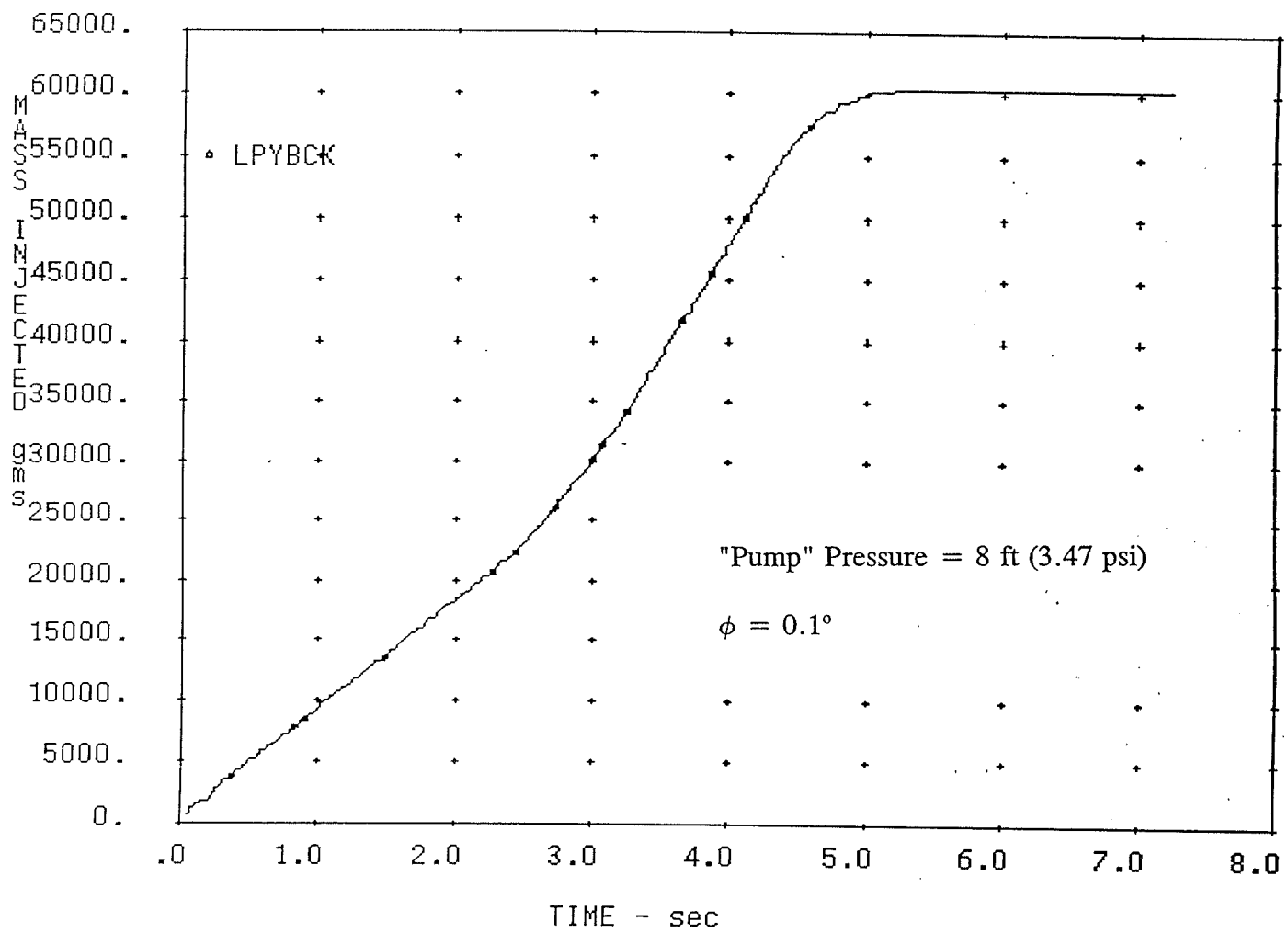


Figure 5a.

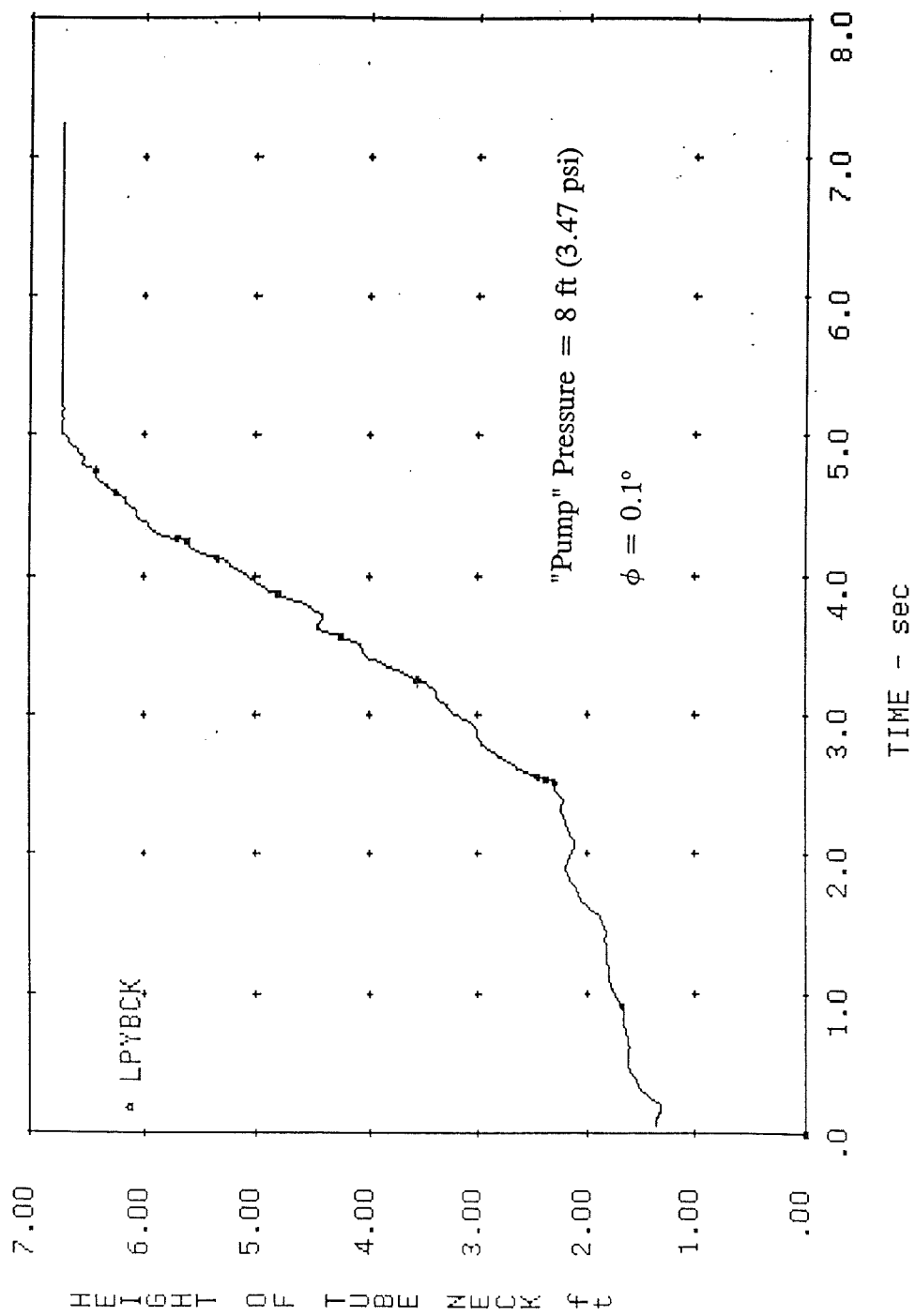


Figure 5b.

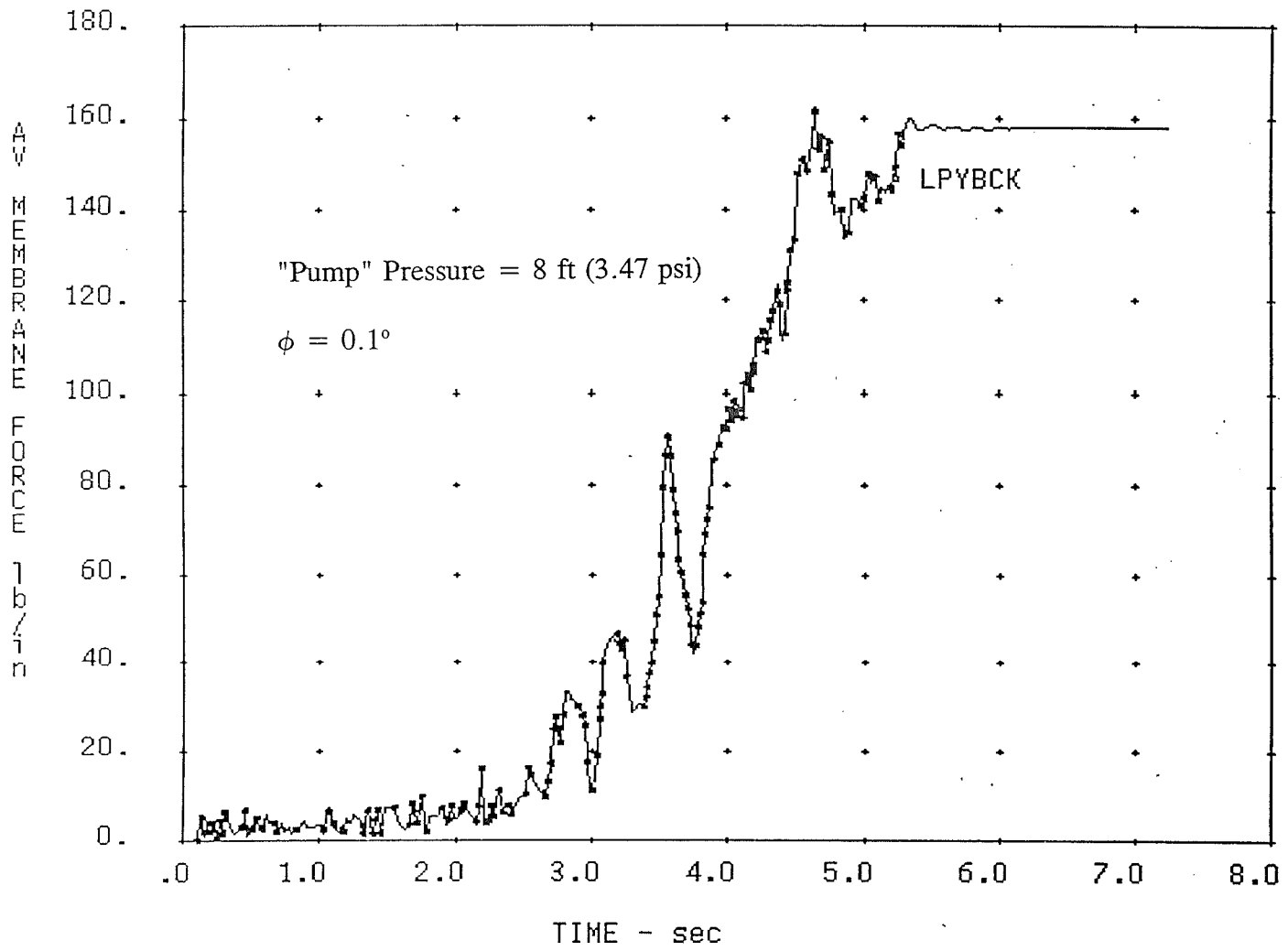


Figure 5c.

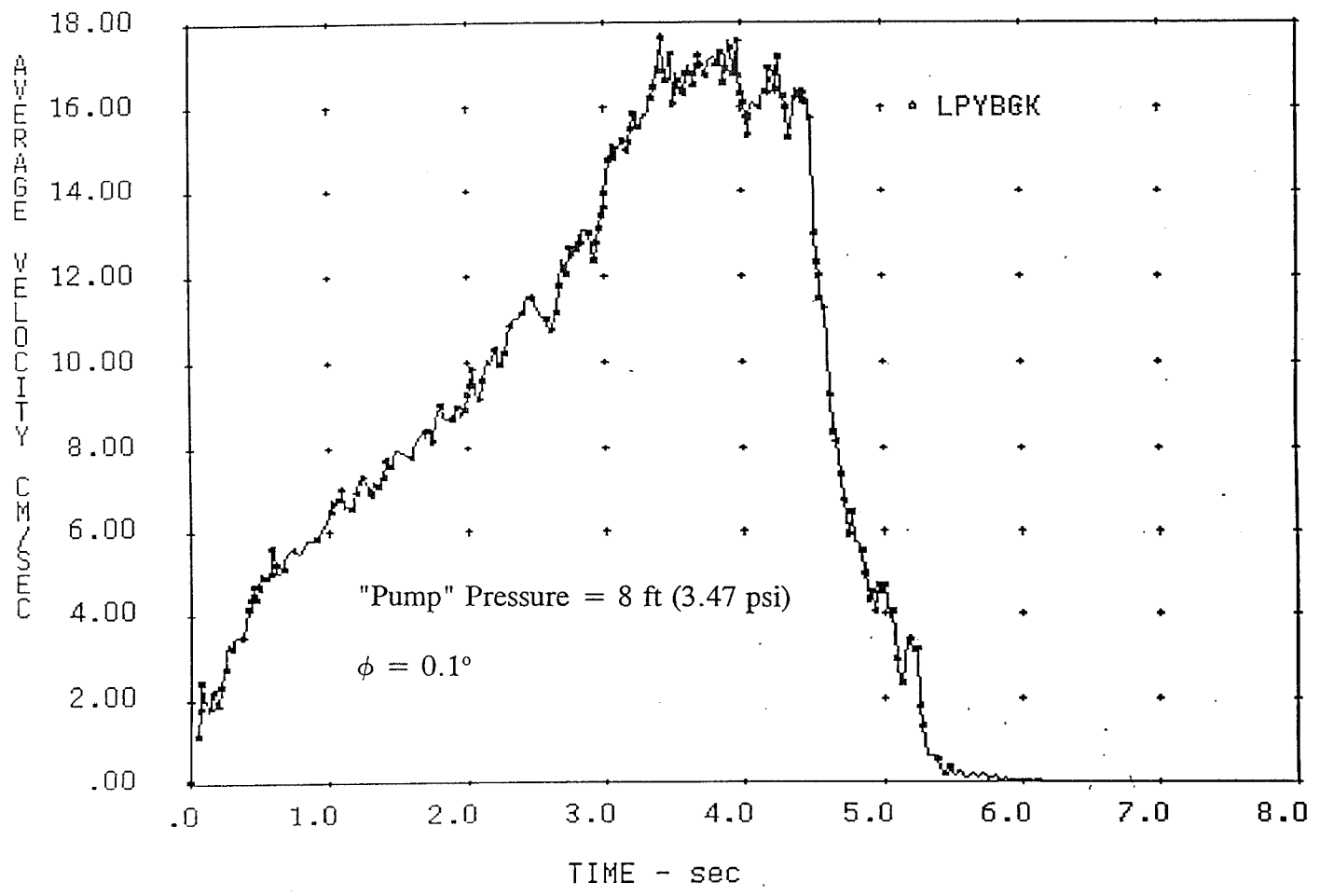


Figure 5d.

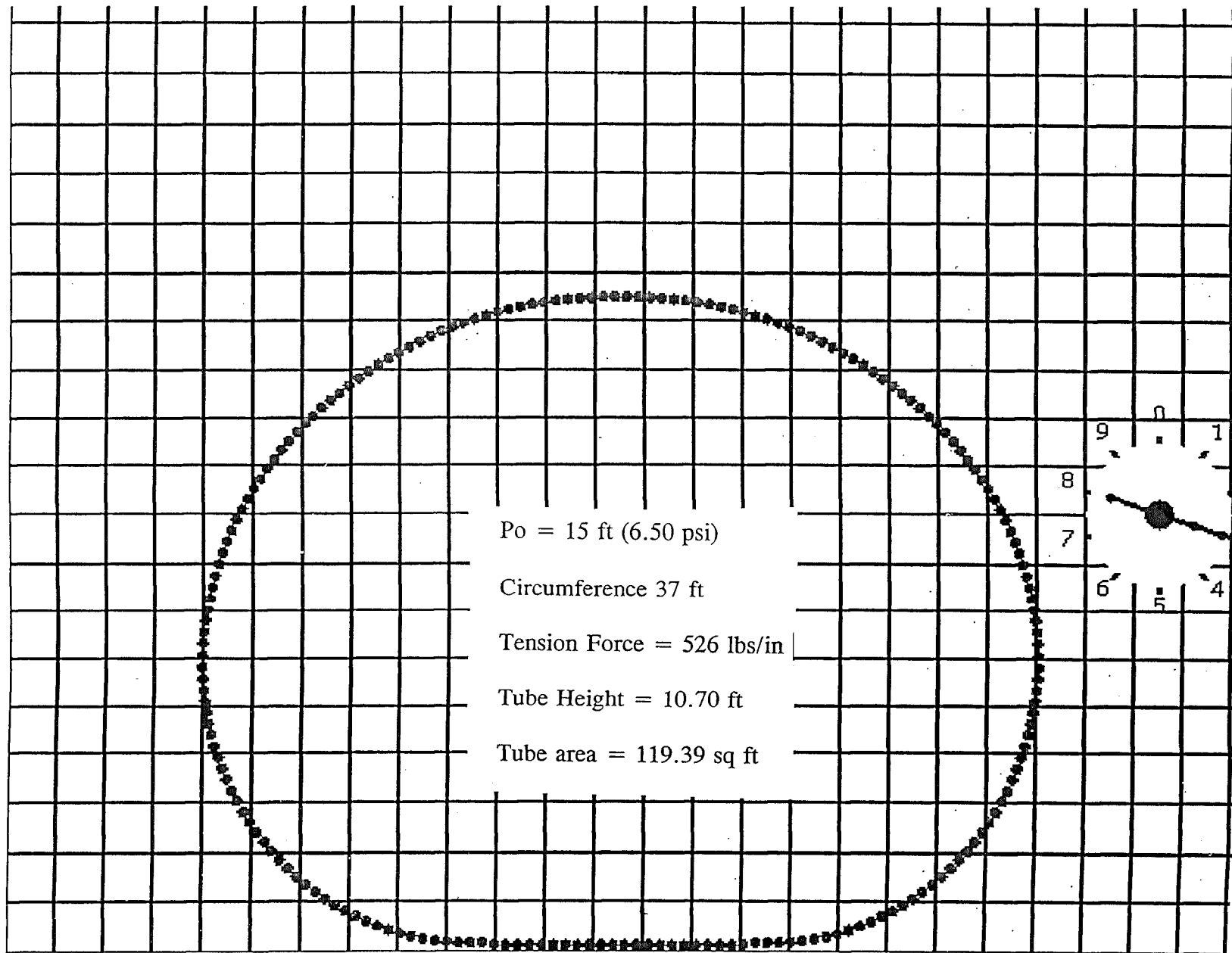


Figure 6.

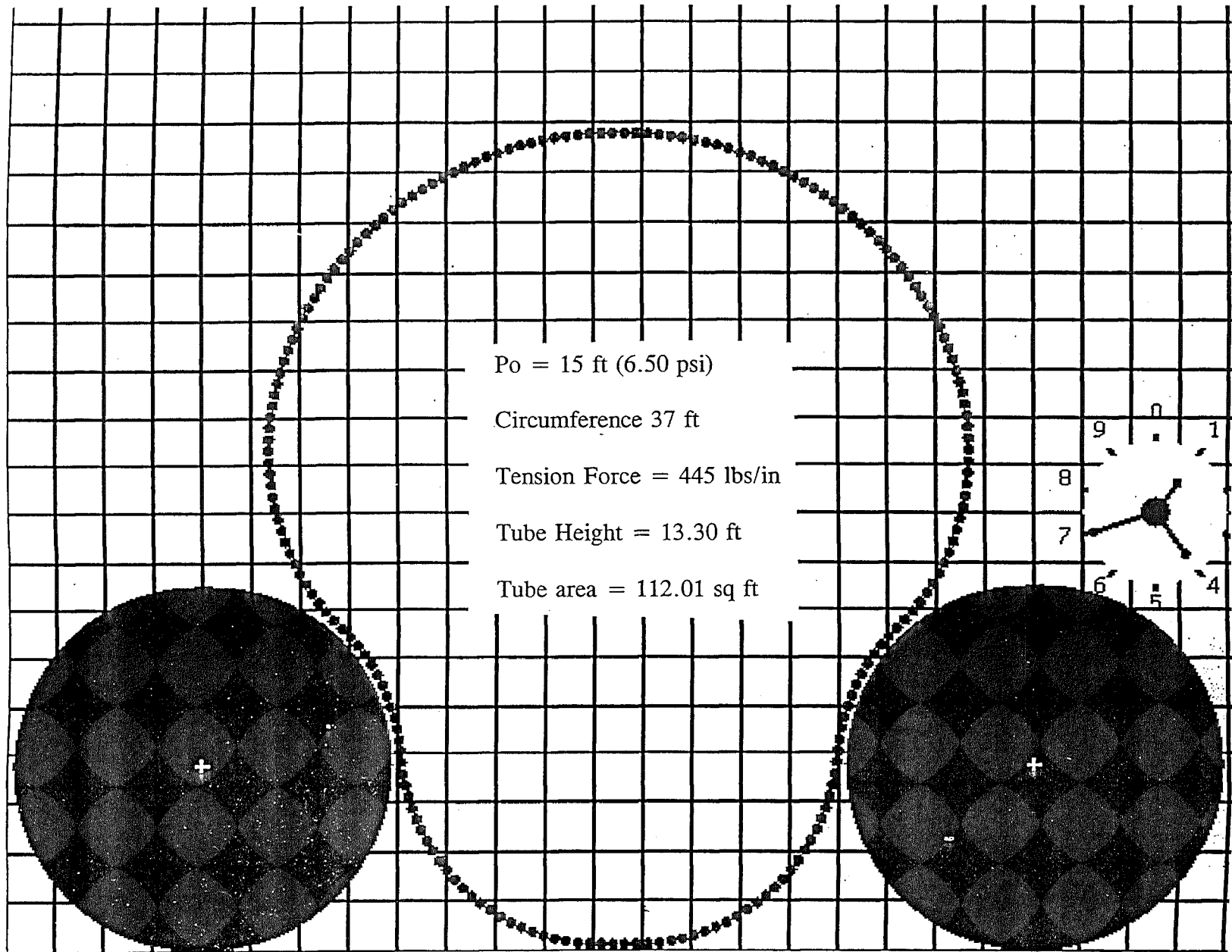


Figure 7a.

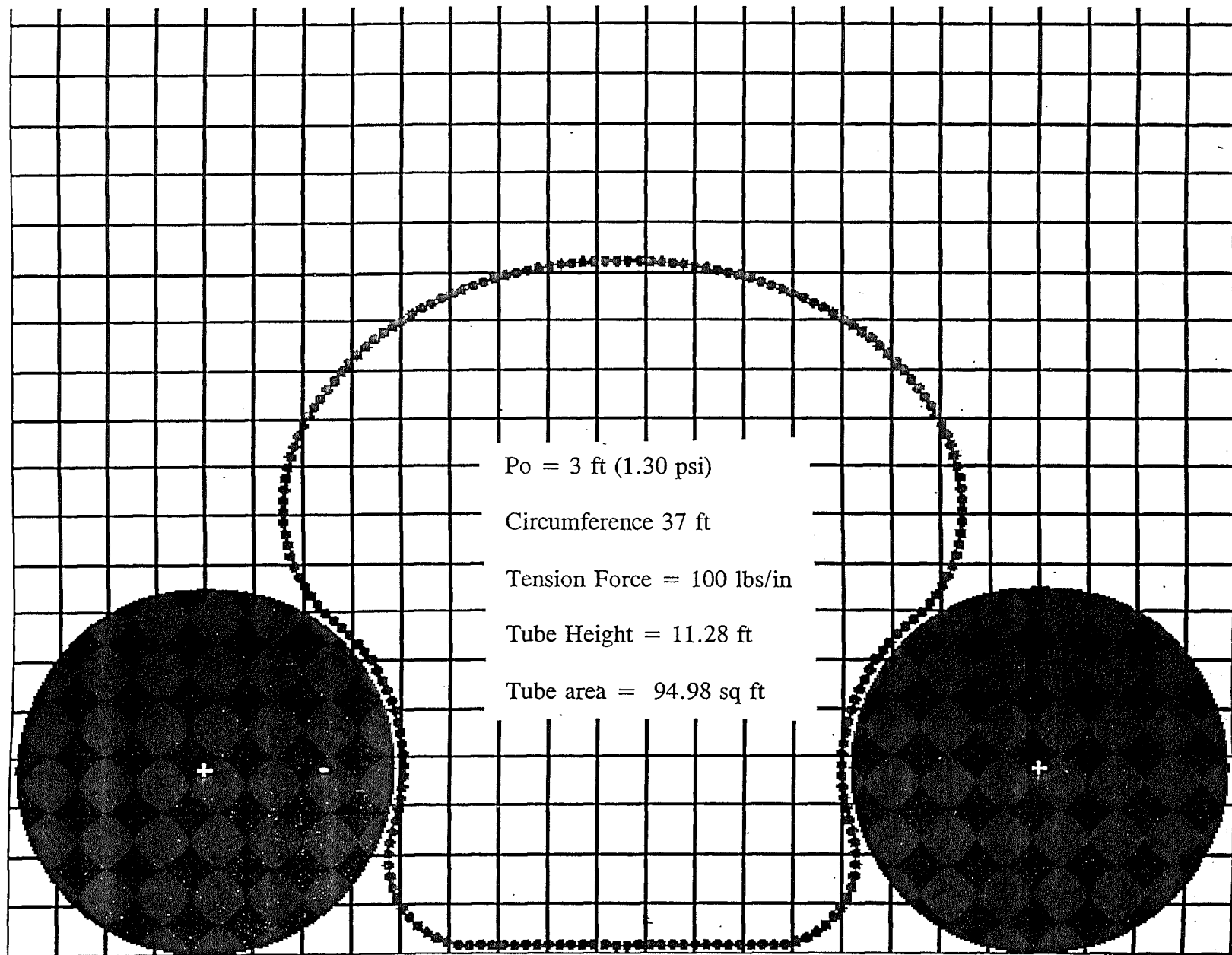


Figure 7b.

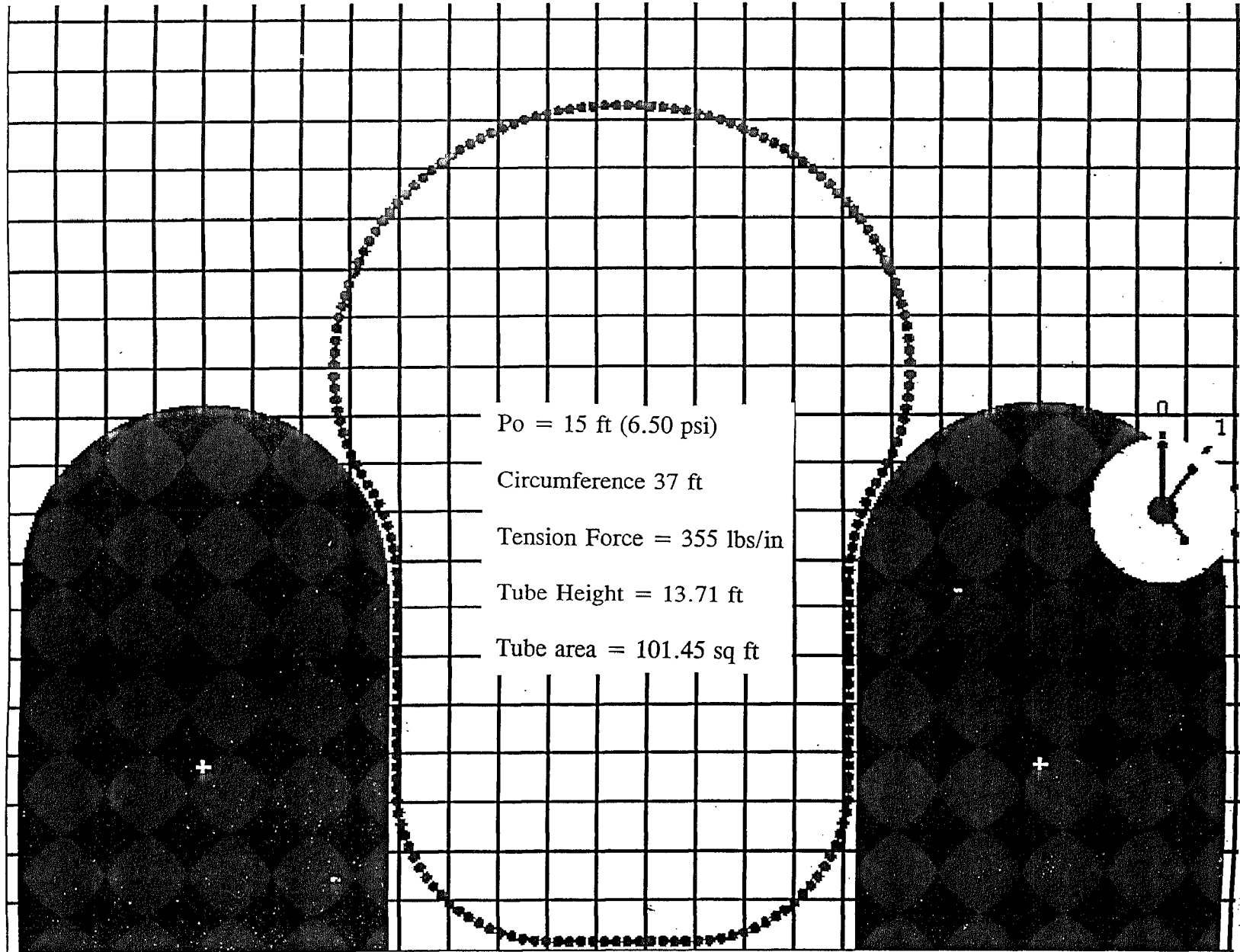


Figure 8a.

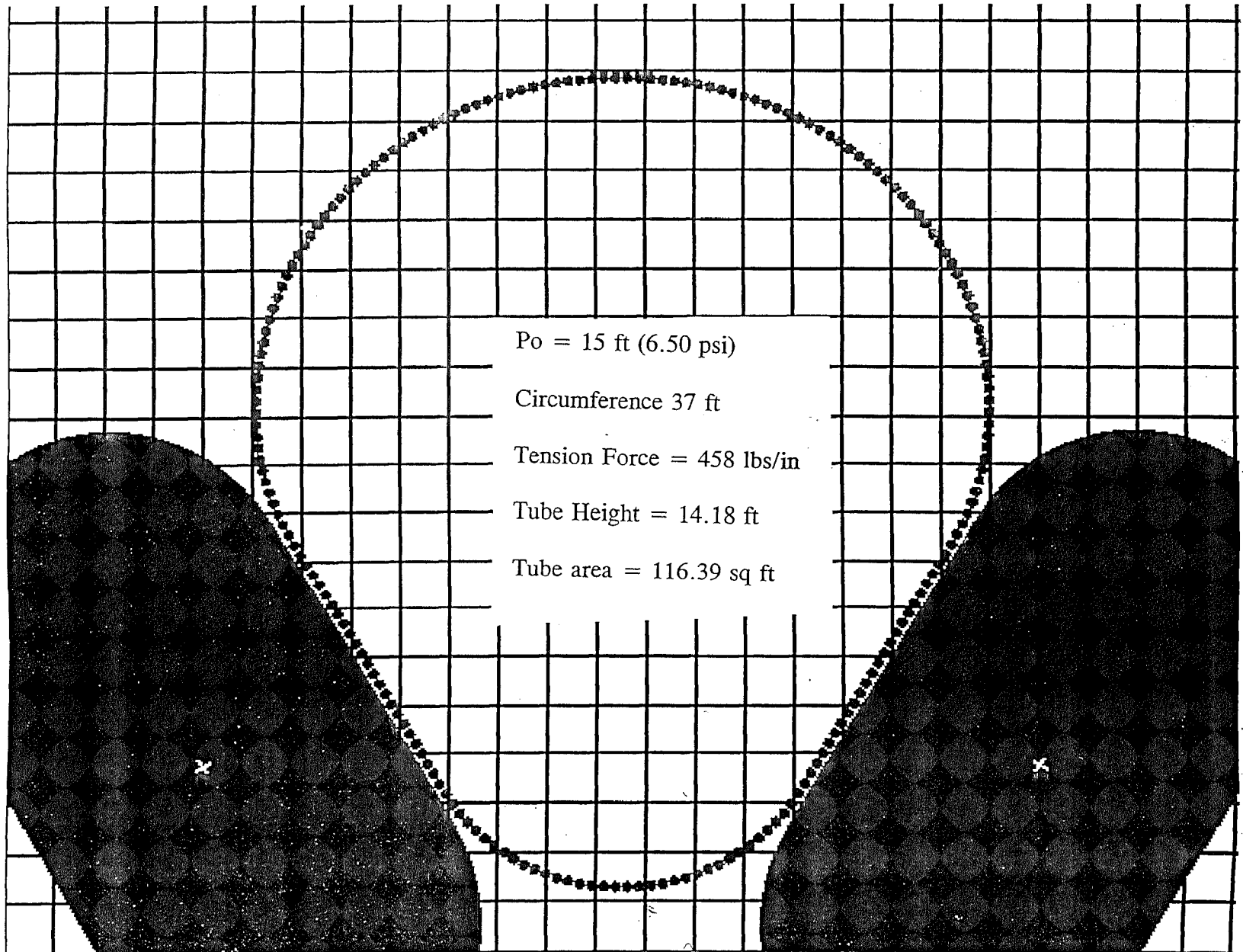


Figure 8b.